

# Synthesis and Characterization of Bodipy-FL-Cyclosporine A as a Substrate for Multidrug Resistance-Linked P-Glycoprotein (ABCB1)<sup>§</sup>

Andaleeb Sajid,<sup>1</sup> Natarajan Raju,<sup>1</sup> Sabrina Lusvarghi, Shahrooz Vahedi, Rolf E. Swenson, and Suresh V. Ambudkar

Laboratory of Cell Biology, Center for Cancer Research, National Cancer Institute (A.S., S.L., S.V., S.V.A.), and Imaging Probe Development Center, National Heart, Lung and Blood Institute (N.R., R.E.S.), National Institutes of Health, Bethesda, Maryland

Received April 25, 2019; accepted July 24, 2019

## ABSTRACT

Fluorescent conjugates of drugs can be used to study cellular functions and pharmacology. These compounds interact with proteins as substrates or inhibitors, helping in the development of unique fluorescence-based methods to study *in vivo* localization and molecular mechanisms. P-glycoprotein (P-gp, ABCB1) is an ATP-binding cassette (ABC) transporter that effluxes most anticancer drugs from cells, contributing to the development of drug resistance. To study the transport function of P-gp, we synthesized a Bodipy-labeled fluorescent conjugate of cyclosporine A (BD-CsA). After synthesis and characterization of its chemical purity, BD-CsA was compared with the commonly used 7-nitrobenz-2-oxa-1,3-diazol-4-yl (NBD)-CsA probe. In flow cytometry assays, the fluorescence intensity of BD-CsA was almost 10 times greater than that of NBD-CsA, enabling us to use significantly lower concentrations of BD-CsA to achieve the same fluorescence levels. We found that BD-CsA is recognized as a transport substrate by both human and mouse P-gp. The rate of efflux of BD-CsA by human P-gp is comparable to that of NBD-CsA. The transport of BD-CsA was inhibited by tariquidar, with similar IC<sub>50</sub> values to those for NBD-CsA. BD-CsA and NBD-CsA both partially inhibited the ATPase activity of P-gp with similar IC<sub>50</sub> values. *In silico* docking of BD-CsA

and NBD-CsA to the human P-gp structure indicates that they both bind in the drug-binding pocket with similar docking scores and possibly interact with similar residues. Thus, we demonstrate that BD-CsA is a sensitive fluorescent substrate of P-gp that can be used to efficiently study the transporter's localization and function *in vitro* and *in vivo*.

## SIGNIFICANCE STATEMENT

The goal of this study was to develop an effective probe to study drug transport by P-glycoprotein (P-gp). Fluorophore-conjugated substrates are useful to study the P-gp transport mechanism, structural characteristics, and development of its inhibitors. Cyclosporine A (CsA), a cyclic peptide comprising 11 amino acids, is a known substrate of P-gp. P-gp affects CsA pharmacokinetics and interactions with other coadministered drugs, especially during transplant surgeries and treatment of autoimmune disorders, when CsA is given as an immunosuppressive agent. We synthesized and characterized Bodipy-FL-CsA as an avid fluorescent substrate that can be used to study the function of P-gp both *in vitro* and *in vivo*. We demonstrate that Bodipy-FL-conjugation does not affect the properties of CsA as a P-gp substrate.

## Introduction

The study of drug resistance mechanisms in cancer cells led to the identification of P-glycoprotein (P-gp; ABCB1), an ABC-transporter efflux pump (Juliano and Ling, 1976; Shen et al., 1986). In the last three decades, numerous studies have elucidated the functional mechanism

and structure of P-gp but with limited success. P-gp is a highly conserved protein, with homologs present in various species, from mice and zebrafish to *Caenorhabditis elegans*. In humans, P-gp is expressed on the epithelial cells of the liver, kidney, placenta, testes, and adrenal gland and on endothelial cells of the blood-brain barrier (Thiebaut et al., 1987; Cascorbi, 2011). The primary function of this transporter is to efflux toxic metabolites and xenobiotics from cells. Because of its functional requirement, P-gp has evolved to be polyspecific, with the ability to transport a wide range of amphipathic and hydrophobic compounds. As a consequence, P-gp can also transport a variety of anticancer drugs out of cells, and its overexpression leads to the development of drug resistance (Ambudkar et al., 1999; Gutmann et al., 2010; Chufan et al., 2015).

This research was funded by the Intramural Research Program of the National Institutes of Health, the National Cancer Institute, Center for Cancer Research and the National Heart, Lung and Blood Institute.

<sup>1</sup>A.S. and N.R. contributed equally to this work.

<https://doi.org/10.1124/dmd.119.087734>.

§ This article has supplemental material available at [dmd.aspetjournals.org](http://dmd.aspetjournals.org).

**ABBREVIATIONS:** ABC, ATP-binding cassette; BD-CsA, Bodipy-FL conjugate of cyclosporine A; Boc, *tert*-butyloxycarbonyl; Bodipy NHS ester, boron, [1-[3-[5-[(3,5-dimethyl-2H-pyrrol-2-ylidene-.N)methyl]-1H-pyrrol-2-yl-.x.N]-1-oxopropoxy]-2,5-pyrrolidinedionato]difluoro; CsA, cyclosporine A; DCM, dichloromethane; DMAP, 4-N,N-dimethylaminopyridine; EDC.HCl, N-(3-dimethylaminopropyl)-N'-ethylcarbodiimide hydrochloride; EtOAc, ethyl acetate; FBS, fetal bovine serum; Fmoc, fluorenylmethoxycarbonyl; Fmoc-OSu, N-(9-fluorenylmethoxycarbonyloxy) succinimide; HEK293, human embryonic kidney cell line 293; HPLC, high-performance liquid chromatography; IMEM, Iscove's modified Dulbecco's medium; LC-MS, liquid chromatography-mass spectrometry; MeOH, methanol; NBD-CsA, 7-nitrobenz-2-oxa-1,3-diazol-4-yl conjugate of cyclosporine A; NHS, N-hydroxysuccinimide; P-gp, P-glycoprotein; RT, room temperature; TFA, trifluoroacetic acid.

Structurally, human P-gp contains two transmembrane domains, each having six transmembrane helices and two nucleotide-binding domains, connected by extracellular and intracellular loops. The nucleotide-binding domains bind and hydrolyze ATP, which is critical for conformational changes associated with the translocation of the substrates across the membrane (Ambudkar et al., 1999, 2006; Szöllösi et al., 2018). Recently, the atomic structures of human P-gp bound to paclitaxel in the inward-open (Alam et al., 2019) and ATP-bound E-Q mutant in inward-closed (Kim and Chen, 2018) conformations have been reported.

To understand the mechanism of transport under *in vitro* and *in vivo* conditions, various fluorophore conjugates of drugs have been used that act as substrates of P-gp (Gribar et al., 2000; Shukla et al., 2011; Strouse et al., 2013; Vahedi et al., 2017; Sajid et al., 2018). These conjugated substrates are useful for studying P-gp transport kinetics by flow cytometry. Cyclosporine A (CsA), an immunosuppressive agent, is a cyclic peptide comprising 11 amino acids (Tanaka et al., 1996; Tedesco and Haragsim, 2012). It is often administered to patients undergoing transplant surgeries or treatment of autoimmune disorders, but the dosage must be carefully controlled to avoid side effects. Although many investigators use CsA as an inhibitor or modulator of P-gp, it is also transported by P-gp (Saeki et al., 1993; Chen et al., 1997; Demeule et al., 1998). Interestingly, CsA treatment has been shown to increase the expression of P-gp in rat tissues (Jette et al., 1996), and P-gp is known to affect CsA pharmacokinetics and interactions with other coadministered drugs (Kelly and Kahan, 2002; Dirks et al., 2004; Pawarode et al., 2007; Barbarino et al., 2013; Yigitaslan et al., 2016). Of all the known substrates of P-gp, CsA is unique, being a large cyclic peptide (~1200 Da). Hence, the availability of fluorescent CsA would also help in its characterization, as it is the only representative of this class of drugs.

In this study, we synthesized a Bodipy-conjugated derivative of CsA (BD-CsA). We show that this derivative is a valuable tool to study P-gp transport, as no fluorescent conjugate of CsA is commercially available. Previously, the 7-nitrobenz-2-oxa-1,3-diazol-4-yl (NBD) conjugate of CsA (NBD-CsA) was synthesized and used as a fluorescent substrate (Wenger, 1986; Schramm et al., 1995; Hartz et al., 2010; Storck et al., 2018) (Fig. 1). In the last few years, Bodipy-FL conjugates of several substrates have been used for characterization of the transport function of wild-type P-gp as well as its variants (Weiss et al., 2003;

Chearwae et al., 2004; Shukla et al., 2011; Li et al., 2017; Vahedi et al., 2018) and to assess P-gp's function at the blood-brain barrier using mouse or rat brain capillaries (Hartz et al., 2010). Thus, there has been a need for a stable derivative of a substrate with a high yield of fluorescence to assess the transport function of P-gp, especially in *in vivo* studies using animal models. Given that CsA is a well characterized substrate of P-gp, we synthesized and characterized BD-CsA as a substrate of P-gp and compared it with NBD-CsA. We showed that BD-CsA can be transported by both human and mouse P-gp. The transport was inhibited by tariquidar, a known P-gp inhibitor. We also demonstrate that, owing to its stability and increased fluorescence yield compared with that of NBD-CsA, BD-CsA is useful for labeling live cells at significantly lower concentrations.

## Materials and Methods

### Chemicals

Bodipy-FL-verapamil (BD-verapamil) was purchased from Setareh Biotech (Eugene, OR). NBD-cyclosporine A was generously provided by Drs. Anika Hartz and Björn Bauer, University of Kentucky (Lexington, KY). All remaining chemicals were purchased from Sigma-Aldrich (St. Louis, MO) and Thermo Fisher Scientific (Waltham, MA), unless otherwise specified.

### Chemical Synthesis of Bodipy-FL-CsA

A schematic representation of the synthesis of BD-CsA is presented in Fig. 2.

**General Procedures.** All analytical high-performance liquid chromatography (HPLC) was run on an Agilent 1200 analytical instrument (Agilent Technologies, Inc., Santa Clara, CA). Water (A) and acetonitrile (B) were used as mobile phases with 0.1% trifluoroacetic acid (TFA) (v/v). Liquid chromatography-mass spectrometry (LC-MS) data were obtained from an Agilent 1200 analytical HPLC and an Agilent Quadrupole 6130 LC-MS. Preparative HPLC was performed using a Shimadzu preparative instrument (Shimadzu Corp., Kyoto, Japan). Chromatographic purifications were carried out using a Teledyne ISCO (Lincoln, NE) flash chromatography system. Analytical HPLC conditions were the following: **I:** Column, Agilent Zorbax-SB300 RP; 5.0  $\mu\text{m}$ ; 3.5  $\times$  50 mm; 1.0 ml/min; detection at 220 nm; 50%–100% gradient B over 5.0 minutes and kept at 100% B for 5 additional minutes. **II:** Same column conditions as in **I**, 70%–100% gradient B over 5 minutes. **III:** Same column conditions as in **I**, 50%–100% gradient B over 10 minutes. **IV:** Column: Waters X Bridge OBD protein BEH-C4 RP Waters Corporation, Milford, MA), 3.5  $\mu\text{m}$ , 300  $\text{\AA}$ , 4.6  $\times$  50 mm; solvent A, water; solvent B, methanol (MeOH); elution rate: 1.5 ml/min; detection at 480 nm; 50%–100% gradient B over 10 minutes.

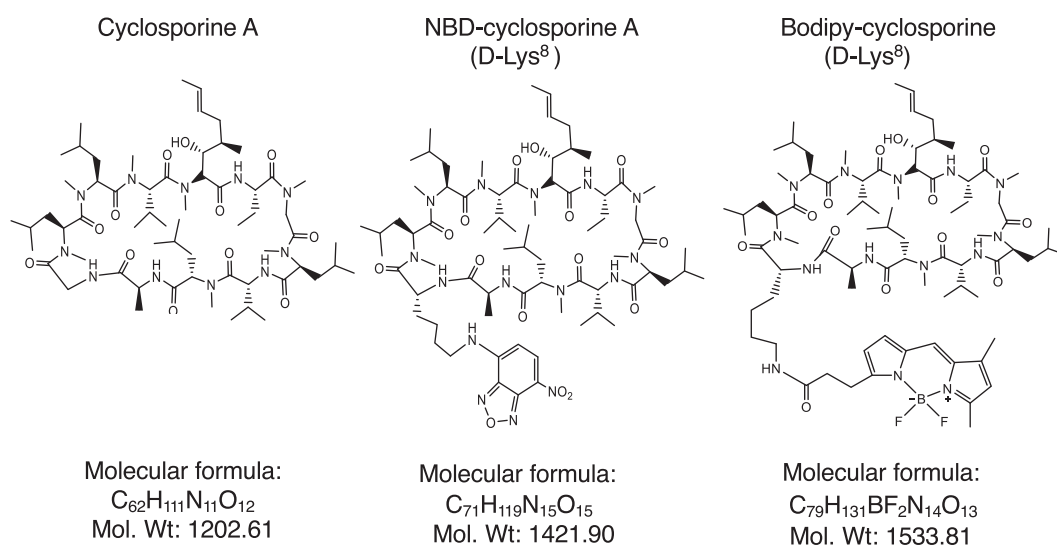


**Fig. 1.** Chemical structures of cyclosporine A and its NBD- and Bodipy-fluorescent conjugates. Diagrams showing chemical structures, formula and molecular weights of cyclosporine A, NBD-cyclosporine A, and BD-cyclosporine A. The fluorescent conjugate was linked to the D-Lys8 residue of a cyclosporine A cyclic peptide.

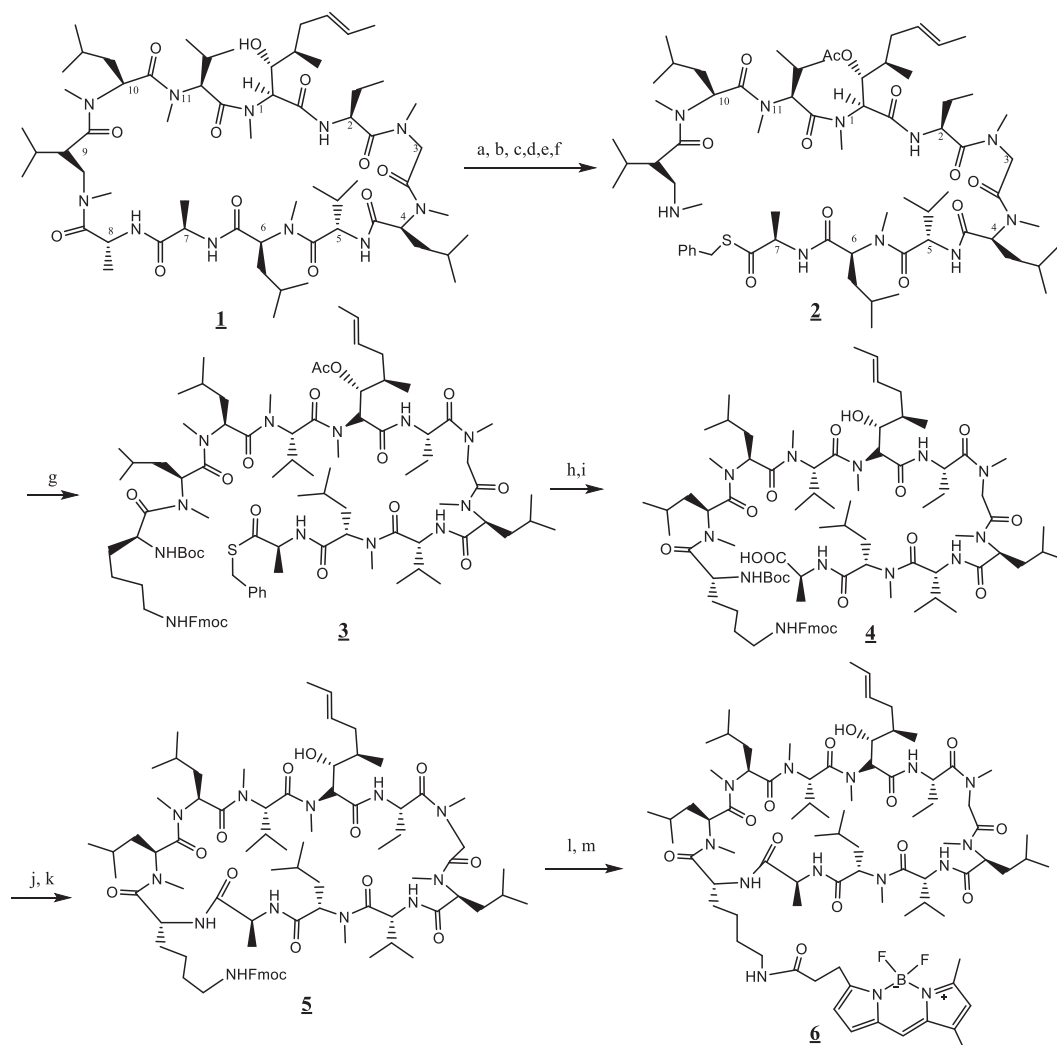


**Fig. 2.** Scheme for the synthesis of Bodipy-FL-cyclosporine A. (a) Pyridine, Ac<sub>2</sub>O, DMAP, 20 hours, RT; (b) P<sub>4</sub>S<sub>10</sub>-pyridine complex, CH<sub>3</sub>CN, reflux, 30 minutes; (c) BnBr, 1,8-diazabicyclo(5,4,0)-undec-7-ene, DCM, 2 hours; (d) 6N HCl, CH<sub>3</sub>CN, RT, 1 hour; (e) PhNCS, CH<sub>3</sub>CN, RT, 4 hours; (g) Boc-D-Lys(Fmoc)-OH, EDC.HCl, DCM, RT, 20 hours; (h) 0.2 N NaOH, MeOH, RT, 72 hours; (i) Fmoc-OSu, THF, RT, 20 hours; (j) 50% TFA in DCM, 30 minutes; (k) *n*-propylphosphonic anhydride, DMAP, DCM, 72 hours; (l) 50% diethylamine in CH<sub>3</sub>CN, RT, 30 minutes; (m) Bodipy-NHS ester, DMF, RT, 20 hours.

**Thionation of Cyclosporine A Acetate; Product 2.** Pyridine-P<sub>4</sub>S<sub>10</sub> complex (Bergman et al., 2011) (0.642 g, 1.69 mmol) was added to a solution of the cyclosporine A acetate (**1**, 7.0 g, 5.63 mmol) in anhydrous acetonitrile (50.0 ml) and refluxed for 30.0 minutes under argon. The solution was cooled and concentrated to 15.0 ml and then diluted with 100.0 ml of water and extracted with 5 × 20.0 ml of ethyl acetate (EtOAc). The combined organic extracts were dried (MgSO<sub>4</sub>), filtered, and concentrated, and the residue was chromatographed over 330.0 g of prepacked silica gel column (50.0 μm). Elution with 1:1 EtOAc/hexanes yielded 7-thioamide (checked by LC-MS), followed by unreacted starting material on continued elution with 6:4 EtOAc/hexanes. Yield was 1.2 g (16.8%, 0.95 mmol, colorless gum); recovered starting material was 5.0 g (4.03 mmol, 71.2%). HPLC conditions **I**, t<sub>R</sub> 4.5 minutes; MS [M + H] was 1261.9. We observed the following: 1) the procedure using phosphorous pentasulfide in xylenes (Eberle and Nüniger, 1993) repeatedly yielded a mixture of positional isomeric thioamides (Fig. 2, structure **1**) 7 (required monothioamide), 4 (unwanted monothioamide), and 4,7-bis thioamide (major side product), which were difficult to separate, along with other products; and 2) the preceding procedure consistently yielded the required 7-isomer and occasionally the 4-isomer, which could be removed at later stages with ease, and no bis isomer was detected by LC-MS. The starting material was recovered (70%–75%) and recycled.

**Coupling of Edman Degradation Product 2 with D-Lysine; Intermediate 3.** EDC.HCl (0.77 g, 4.0 mmol) was added to a mixture of Boc-D-Lys (fluorenylmethoxycarbonyl, Fmoc)-OH (1.4 g, 3.0 mmol) and amine **2** (1.3 g, 1.0 mmol)

in anhydrous dichloromethane (DCM) (20.0 ml) and stirred for 20 hours at room temperature (RT). The reaction mixture was concentrated under reduced pressure, and the residue was purified over 100.0 g of prepacked flash silica gel column (25–50.0 μm). Elution with 0%–10% MeOH in DCM eluted the required peptide at 8% MeOH concentration. The LC fractions with the pure product were pooled and concentrated to yield the fully protected linear peptide as a colorless foam. Yield was 0.97 g (55%, 0.55 mmol); HPLC conditions were **I**, t<sub>R</sub> 5.3 minutes, and MS was [M + Na] 1771.1.

**D-Lys<sup>8</sup>-Cyclosporine 5.** Compound **3** (1.94 g, 1.5 mmol) was dissolved in a mixture of 0.2 M NaOH in water (22.5 ml) and MeOH (25.0 ml) and stirred at RT for 72 hours. The solution was concentrated under reduced pressure to 10.0 ml, and the pH was adjusted with 0.2 M of NaHSO<sub>4</sub> to 8.0. Fmoc-OSu (0.68 g, 2.0 mmol); THF (10 ml) was added and stirred at RT for 20 hours. The solution was concentrated under reduced pressure to 15.0 ml, and then the pH was adjusted with 0.2 M NaHSO<sub>4</sub> to 3.0. The reaction mixture was diluted with water (50.0 ml) and extracted with 5 × 30 ml of DCM. The combined organic layer was washed with water, dried (Na<sub>2</sub>SO<sub>4</sub>), filtered, concentrated, and purified by C18 RP flash silica gel column (120.0 g, solvent A, water; solvent B, MeOH; 0%–100% B over 60 minutes; elution rate, 60 ml/min; detection at 220 and 280 nm). Fractions with the compound and purity of >90% were (LC-MS) were pooled and concentrated to yield the acid **4** as a colorless gum. Yield was 0.98 g, (40%, 0.61 mmol), MS [M + Na] 1622.7. This acid (150.0 mg, 0.094 mmol) was dissolved in 50% TFA in DCM (20 ml) and kept at RT for

30 minutes. All the volatiles were removed under reduced pressure, and the residue was dried under high vacuum for 2 hours. The crude amino acid (0.113 g, 0.07 mmol) in anhydrous DCM (300.0 ml), *n*-propyl phosphonic anhydride (44.5 mg, 50% in EtOAc, 90.0  $\mu$ l, 0.21 mmol), and DMAP (68.0 mg, 0.56 mmol) were stirred under argon for 72 hours at RT. The solution was concentrated under reduced pressure, and the residue was purified on a flash C18 RP column (275.0 g; 25.0  $\mu$ m; A, water; B, MeOH; elution rate: 80 ml/min; detection at 220 nm and 280 nm; 0%–100% B over 100 minutes). The fraction with the required mass and purity >90% were pooled and concentrated under reduced pressure to **5** as a colorless foam. Yield was 51.6 mg (49%, 0.034 mmol). HPLC conditions: **III**;  $t_R$  5.2 minutes, and MS [M + H] was 1482.9.

**Bodipy Fl-D-Lys<sup>8</sup>-Cyclosporine (BD-CsA) 6.** [N<sup>ε</sup>-Fmoc]-D-Lys<sup>8</sup>-cyclosporine **5** (100.0 mg; 0.0625 mmol) was dissolved in 50% diethylamine in acetonitrile (20.0 ml) and kept at RT for 30.0 minutes. All the volatiles were removed under reduced pressure, and the residue was coevaporated with toluene (3  $\times$  10 ml). The deprotected amine (above) in anhydrous DMF (3.0 ml) was stirred with Bodipy N-hydroxysuccinimide (NHS) ester obtained from A1 Biochem Laboratories (Wilmington, NC) (32.3 mg, 0.07 mmol), under argon protected from light for 24 hours. DMF was evaporated under reduced pressure, and the residue was purified by preparative HPLC [conditions: column: Waters Corporation X-Bridge protein BEH-C4 RP; 5.0  $\mu$ m; 300 Å; 19  $\times$  150 mm; detection at 480 nm; solvent A, water; solvent B, MeOH; 20% B to 100% over 40.0 minutes; elution rate: 30 ml/min]. Fractions with >95% purity were pooled and concentrated under reduced pressure at RT to yield the product as a brown gum. Yield: 51.8 mg (52.8%, 0.033 mmol). Analytical HPLC conditions, **iv**;  $t_R$  4.3 minutes; MS [M + H] 1534.3.

#### Cell Lines and Culture Conditions

HeLa cells were obtained from American Type Culture Collection (Manassas, VA). Cells were maintained in Dulbecco's modified Eagle's medium (Difco Laboratories, Detroit, MI) supplemented with 10% fetal bovine serum (FBS), 5 mM L-glutamine, 100 U/ml penicillin, and 100  $\mu$ g/ml streptomycin at 37°C in 5% CO<sub>2</sub>.

#### Recombinant BacMam and Baculovirus Generation

The Bac-to-Bac Baculovirus Expression system (Life Technologies, Carlsbad, CA) was used to generate recombinant baculovirus and BacMam baculovirus, as described previously (Pluchino et al., 2016). Briefly, human *MDR1* and mouse *ABCB1a* and *ABCG2* genes were cloned in pDonr-255 and used for Gateway cloning into pDest-625 (mammalian cell expression) and pDest-008 (insect cell expression). pDest clones were transformed in *Escherichia coli* DH10Bac competent cells and used to prepare the recombinant Bacmids for generation of BacMam and baculovirus according to the manufacturer's protocol (Gibco: ThermoFisher).

#### BacMam Baculovirus Transduction of HeLa Cells and Transport of Fluorescent Substrates

HeLa cells were transduced with human P-gp, mouse P-gp, or human ABCG2 BacMam baculovirus, as described previously (Shukla et al., 2012; Vahedi et al., 2017; Sajid et al., 2018). Briefly, HeLa cells were incubated with the BacMam baculovirus at a selected cell:virus ratio for 4 hours. Sodium butyrate (10 mM) was added, and incubation was continued for an additional 12–16 hours at 37°C in 5% CO<sub>2</sub>. For transport assays of P-gp, transduced HeLa cells were trypsinized and resuspended in Iscove's modified Dulbecco's medium (IMDM) containing 5% FBS; 3  $\times$  10<sup>5</sup> cells were incubated with fluorescent substrates (BD-verapamil, pheophorbide A, BD-CsA, or NBD-CsA) at selected concentrations for 45 minutes at 37°C. After incubation, cells were washed with cold IMDM and resuspended in cold PBS containing 1% BSA. The transport of substrates was measured by flow cytometry using untransduced cells as a control. The mean fluorescence intensity of P-gp-expressing cells after subtraction from that of untransduced cells (not expressing P-gp) was taken as 100% efflux. For inhibition assays, tariquidar (200 nM for steady-state assay and 0–100 nM for IC<sub>50</sub> calculations) was added wherever indicated. Both NBD-CsA and BD-CsA were tested with ABCG2-expressing HeLa cells and MRP1-expressing human embryonic cell line HEK293 cells as described below. To test the transport activity of ABCG2, pheophorbide A (a substrate) was used at 2  $\mu$ M and Ko143 (an inhibitor) at 2.5  $\mu$ M. HEK-MRP1 and HEK-PCDNA3.1 (vector control) cell lines were used

to determine the transport activity of human MRP1 (Müller et al., 2002), with calcein-AM/NBD-CsA/BD-CsA (0.25  $\mu$ M) and the inhibitor MK571 (25  $\mu$ M). Flow cytometry was done using a FACS CANTO II instrument with BD FACSDiva software (BD Biosciences, BD Biosciences, San Jose, CA), and spectra were collected in the fluorescein isothiocyanate region (Ex. 488 nm, Em. 525 nm). The data were analyzed using FlowJo software (Tree Star, Inc., Ashland, OR).

#### Time Course of Efflux of BD-CsA and NBD-CsA

HeLa cells were transduced with BacMam baculovirus as described earlier (Sajid et al., 2018). After trypsinization, cells were resuspended in PBS containing 1 mM MgCl<sub>2</sub> and 0.1 mM CaCl<sub>2</sub>. For depletion of ATP, 2-deoxyglucose (20 mM) and sodium azide (5 mM) were added, and cells were incubated at 37°C for 10 minutes. Substrates (BD-CsA or NBD-CsA, 0.5  $\mu$ M) were added to the cells and incubated at 37°C for another 20 minutes to load the cells. After incubation, cells were washed with cold PBS/Ca<sup>2+</sup>/Mg<sup>2+</sup>, and IMDM + 5% FBS (enriched medium) was added, followed by incubation at 37°C for different time points (0, 1, 2, 5, 10, 20, and 30 minutes). Cells were washed with cold IMDM, and PBS + 1% BSA was added to be used for analysis by flow cytometry. The time required for 50% ( $T_{1/2}$  min) efflux of BD-CsA or NBD-CsA was calculated using GraphPad Prism version 7.0 (GraphPad Software, San Diego, CA).

#### Fluorescence Microscopy-Based Transport Assay

Transduction was carried out as described in the earlier section using HeLa cells seeded in a 24-well plate format (50,000 cells/well). After 20–22 hours, cells were washed twice with PBS, and fluorescent substrates (BD-CsA or NBD-CsA) were added at 0.5  $\mu$ M concentration in 1 ml IMDM containing 5% FBS. Tariquidar (200 nM) was added to the samples wherever indicated. Untransduced cells were used as a control. The transport assay was carried out for 45 minutes at 37°C. Ten minutes before completion of the transport assay, NucBlue Live cell stain (Invitrogen, Carlsbad, CA) was added to the cells. The cells were washed with cold PBS three times, and 0.5 ml of PBS was added to each well. Live cells were visualized in an Evos AMG microscope at 10 $\times$  magnification in transmitted light (to visualize the cells), green fluorescent protein region (for fluorescence of BD-CsA and NBD-CsA) and UV-blue region (to visualize stained nuclei with NucBlue).

#### Preparation of Total Membranes from High Five Insect Cells

The *ABCB1* gene cloned in pDEST-008 was transformed in *E. coli* DH10Bac cells, and bacmids were prepared harboring recombinant P-gp with a 6X His-tag and TEV-cleavage site at the C-terminal end, as described previously (Vahedi et al., 2017). High Five insect cells (Invitrogen) were infected with recombinant baculovirus carrying P-gp. Membrane vesicles were prepared by hypotonic lysis of the insect cells, followed by ultracentrifugation to collect the membrane vesicles (Ramachandra et al., 1998; Kerr et al., 2001).

#### ATPase Assay

ATP hydrolysis was measured using membrane vesicles of High Five insect cells expressing P-gp, as described previously (Sajid et al., 2018). Membrane vesicles (10  $\mu$ g of protein per 100  $\mu$ l of reaction volume) were incubated in the presence or absence of 0.3 mM sodium orthovanadate in ATPase assay buffer (50 mM MES-Tris pH 6.8, 50 mM KCl, 10 mM MgCl<sub>2</sub>, 5 mM Na<sub>3</sub>, 1 mM EGTA, 1 mM ouabain, and 2 mM DTT). Basal ATPase activity was measured in the presence of DMSO, and drug-modulated activity was measured in the presence of selected drugs (drug stocks prepared at a 100 $\times$  concentration in DMSO). The reaction was started at 37°C by the addition of 5 mM ATP and stopped by the addition of 2.5% sodium dodecyl sulfate after a 20-minute incubation. The level of generated inorganic phosphate was quantified with a colorimetric method (Ramachandra et al., 1998; Vahedi et al., 2017). The vanadate-sensitive ATPase activities were determined and plotted with GraphPad Prism software (version 7).

#### In Silico Modeling

The recently published ligand (paclitaxel)-bound human P-gp structure (PDB ID: 6QEX) (Alam et al., 2019) was used for docking of CsA, NBD-CsA, and BD-CsA with AutoDock Vina (Scripps Research Institute, La Jolla, CA). For this, the

transporter and ligands were prepared using the MGL tools software package (Scripps Research Institute) (Sanner, 1999; Trott and Olson, 2010). Because AutoDock Vina does not have a Forcefield for boron and given that the Bodipy moiety in BD-CsA has boron in its structure, this atom was treated as carbon for docking purposes. Close examination of published cryo-EM and X-ray structures of mouse and human P-gp (Szewczyk et al., 2015; Nicklisch et al., 2016; Alam et al., 2018, 2019), as well as our docking experiments, allowed us to identify 36 residues that interact with ligands in the drug-binding site. The side chains of these 36 residues, all located in the drug-binding pocket in the transmembrane region of P-gp, were set as flexible. The residues were L65, M68, M69, F72, Q195, W232, F303, I306, Y307, Y310, F314, F336, L339, I340, F343, Q347, N721, Q725, F728, F732, F759, F770, F938, F942, Q946, M949, Y953, F957, L975, F978, V982, F983, M986, Q990, F993, and F994. The receptor grid was centered at  $x = 19$ ,  $y = 53$  and  $z = 3$  and a box with inner box dimensions  $40 \times 40 \times 44 \text{ \AA}$  was used to search for all the possible binding poses within the transmembrane region of the protein. The exhaustiveness level was set at 100 to ensure that the global minimum of the scoring function would be found considering the large box size and the number of flexible residues.

## Results

### Chemical Synthesis of BD-CsA

To develop an efficient and unique probe as a P-gp substrate, we decided to prepare a Bodipy-FL-labeled compound. Previously, NBD-CsA was synthesized as a fluorescent probe (Wenger, 1988), which was used as a reference in this study. The chemical structures of CsA, NBD-CsA, and BD-CsA are shown in Fig. 1. Figure 2 shows a schematic representation of the synthesis of BD-CsA. Commercially available CsA was converted to intermediate **2** as detailed in the literature (Eberle and Nuninger, 1993), except for step *b*. Thioamide formation was accomplished using the pyridine- $P_4S_{10}$  complex (Bergman et al., 2011), instead of phosphorous pentasulfide, yielding a much cleaner reaction product (see experimental details). Intermediate **2** was converted to **3** using standard peptide coupling conditions. Deprotection of **3** and re-protection of  $\epsilon$ -amine of the lysine residue resulted in **4**, which was subjected to intramolecular cyclization to yield the required D-Lysine<sup>8</sup>-cyclosporine protected as its Fmoc-derivative **5**. Removal of the protecting group from **5** followed by conjugation with Bodipy-NHS ester yielded the labeled CsA derivative **6** after preparative HPLC (Supplemental Figs. S1 and S2). The use of Fmoc protection of the  $\epsilon$ -amine of D-lysine allows the introduction of a fluorescent group at the final step. This change

offers the flexibility of conjugation to the fluorescent group or to other groups and simplifies the final purification.

### Comparison of the Fluorescence Intensities of BD-CsA and NBD-CsA

CsA has been widely used in studies of P-gp as an inhibitor or modulator of activity. Even though cyclosporine A is transported by P-gp, because of its relatively high affinity and slow efflux rate, it is often used as an inhibitor of transport (Demeule et al., 1999; Muzi et al., 2009; Jouan et al., 2016). In the past, several groups have characterized the transport of NBD-CsA as a P-gp substrate (Schramm et al., 1995; Masereeuw et al., 2000; Ott et al., 2010; Chufan et al., 2013; Miller, 2014; Vahedi et al., 2017; Sajid et al., 2018). In the present study, we compared BD-CsA and NBD-CsA transport by human P-gp expressed on the surface of HeLa cells. HeLa cells were transduced with BacMam baculovirus expressing human P-gp, and untransduced HeLa cells not expressing detectable levels of P-gp were used as a control. First, the fluorescence intensities of both BD-CsA and NBD-CsA were compared using a concentration gradient of both the probes in the untransduced cells. We found that under the same flow cytometry voltage settings, the intensity of BD-CsA was almost 10 times greater than that of NBD-CsA, with  $0.5 \mu\text{M}$  of NBD-CsA showing the same fluorescence intensity as that of  $0.05 \mu\text{M}$  of BD-CsA (Fig. 3A). The P-gp-expressing cells efflux these substrates, resulting in decreased fluorescence intensity. Next, we calculated the efflux at different concentrations of both probes. As shown in Fig. 3B, the efflux (the difference between the fluorescence intensities of untransduced cells and cells expressing P-gp) was linear, in the range of  $0$ – $0.5 \mu\text{M}$  BD-CsA and NBD-CsA. There was significant efflux for BD-CsA but not NBD-CsA below  $0.5 \mu\text{M}$ . Thus, in subsequent assays, we used  $0.5 \mu\text{M}$  of both the probes to compare their characteristics. Our results showed that BD-CsA has a higher fluorescence yield that can be used to develop more sensitive assays, which is critical in animal studies in which lower doses of BD-CsA can be helpful to avoid toxicity.

### BD-CsA and NBD-CsA Are Transported by Both Human and Mouse P-gp

Using the BacMam baculovirus transduction system, the efflux of NBD-CsA and BD-CsA was compared using HeLa cells transduced with human P-gp (*ABCB1*). We found that human P-gp was able to efflux both

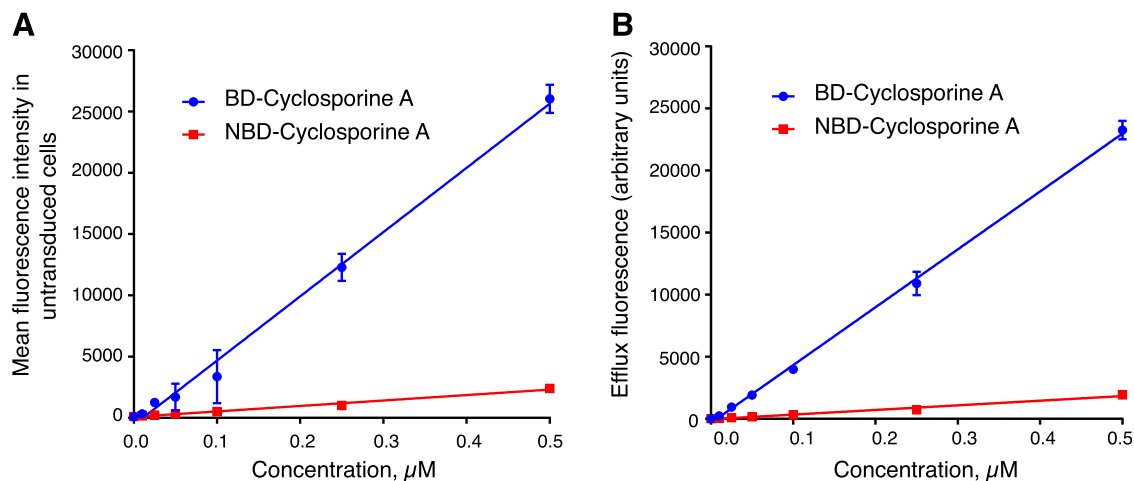


**Fig. 3.** Kinetics of BD-CsA and NBD-CsA accumulation and efflux. HeLa cells were transduced with BacMam baculovirus to express P-gp, and untransduced cells were used as control. Cells were incubated with different concentrations of BD-CsA and NBD-CsA ( $0$ – $0.5 \mu\text{M}$ ) (A) Comparison of fluorescence intensity of BD-CsA with NBD-CsA in untransduced cells. The fluorescence intensity is proportional to the concentration of the substrates but is much higher for BD-CsA compared with NBD-CsA. (B) Efflux of BD-CsA and NBD-CsA calculated by subtracting fluorescence of cells expressing P-gp from that of untransduced cells. The efflux was linear with increasing concentrations of both the substrates but more significant at  $0.5 \mu\text{M}$ . All the experiments were repeated three times; error bars show S.D.

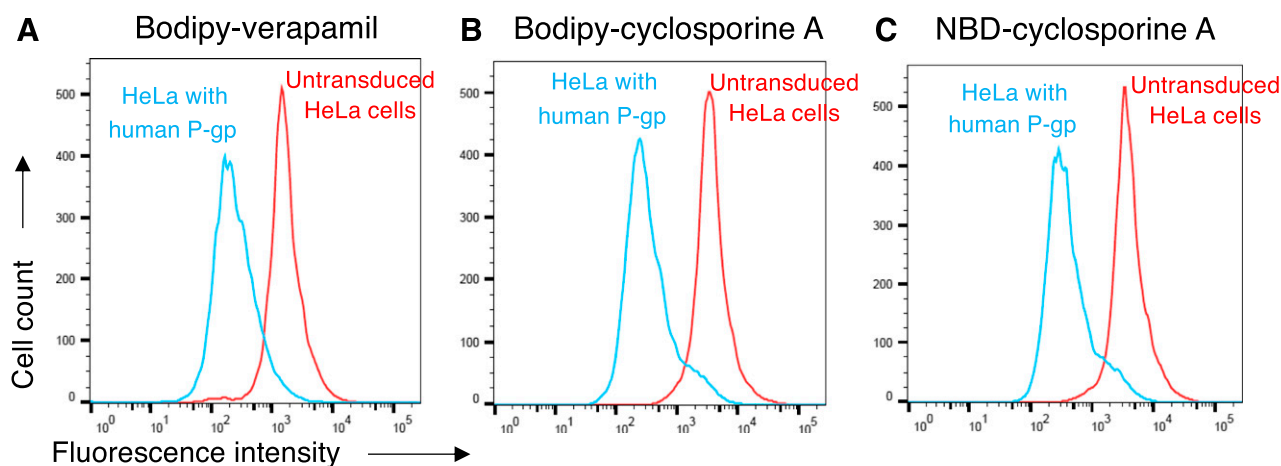


**Fig. 4.** BD-CsA is a substrate of human P-gp. HeLa cells were transduced with BacMam baculovirus to express P-gp, and untransduced cells were used as a control. Cells were incubated with BD-CsA or NBD-CsA (0.5  $\mu$ M, each) for 45 minutes at 37°C, and fluorescence was measured using flow cytometry. Histogram traces show the transport of substrates by human P-gp. (A) BD-verapamil, (B) BD-CsA, and (C) NBD-CsA. The efflux by P-gp was assayed by comparing the fluorescence intensity of cells expressing P-gp (blue traces) with those that do not express P-gp (untransduced cells, red traces).

NBD-CsA and BD-CsA with similar efficiency. BD-verapamil was used as positive control for transport, and the representative transport profiles of BD-verapamil, NBD-CsA, and BD-CsA are shown in Fig. 4. As shown in the histograms, the substrates were transported by P-gp (blue traces), leading to a decreased fluorescence in the cell compared with untransduced cells (red traces).

The mouse homolog of human P-gp (*mdr1a*) has 87% sequence identity. For comparison of transport profiles, mouse P-gp was expressed by using BacMam baculovirus on the surface of HeLa cells, and a transport assay was carried out. As shown in Supplemental Fig. S3, mouse P-gp transports both BD-CsA and NBD-CsA at similar levels as human P-gp. Transport of BD-verapamil as a control is also shown. Since BD-CsA is transported by human and mouse P-gp to the same extent, subsequent experiments were carried out with only human P-gp. We also tested the specificity of these substrates for two other major ABC drug transporters, MRP1 and ABCG2. As shown in Supplemental Fig. S4, ABCG2 does not efflux either BD-CsA or NBD-CsA, although normal efflux of its substrate pheophorbide A was observed. These data are consistent with an earlier report showing lack of transport of NBD-CsA by ABCG2 (Ejendal and Hrycyna, 2005). MRP1 shows marginal efflux of both BD-CsA and NBD-CsA, indicating that fluorescent conjugates of CsA are poor substrates of MRP1 compared with calcein-AM, a known substrate.

#### Comparison of the Rate of Efflux of BD-CsA and NBD-CsA by P-gp

After confirming that BD-CsA and NBD-CsA are transported by P-gp in a steady-state assay, we compared the rate of efflux for both the compounds. HeLa cells were first depleted of ATP, as described in *Materials and Methods*, followed by loading with fluorescent substrates under ATP-depleted conditions. Because of the depletion of ATP, P-gp was not active, and both the substrates diffused in the cells to reach an equilibrium. A time-course efflux assay (0–30 minutes) was performed after the addition of IMDM medium containing glucose. Fluorescence intensity at time 0 (no efflux) was taken as 100%, and relative efflux at indicated time points was calculated. As shown in Fig. 5, the percent remaining BD-CsA and NBD-CsA (minimum remaining in cells) at 30 minutes are almost the same (BD-CsA = 15.3  $\pm$  7.8% and NBD-CsA = 17.3  $\pm$  4.9%; mean  $\pm$  S.D. from three independent experiments), and both BD-CsA and NBD-CsA are effluxed at a similar rate by P-gp with  $T_{1/2}$  of 5.5  $\pm$  1.5 and 3.4  $\pm$  0.7 minutes, respectively. As expected, untransduced cells did not show significant efflux of either substrate (blue and red dashed lines in Fig. 5), showing that the efflux is specifically due to P-gp activity.

#### Tariquidar Inhibits Transport of NBD-CsA and BD-CsA by P-gp

Transport of substrates by P-gp is inhibited by tariquidar (originally known as XR9576) (Martin et al., 1999). To compare the inhibition of efflux of BD-CsA and NBD-CsA by P-gp, tariquidar (200 nM) was added during the transport assay. Figure 6 shows that there is no efflux of either of the compounds in the presence of tariquidar. Subsequently, to test the kinetics of inhibition, tariquidar was used at different concentrations ranging from 0 to 100 nM.  $IC_{50}$  values were calculated from the curve generated using a variable slope nonlinear regression curve fit. The efflux of both the compounds was inhibited by tariquidar with comparable  $IC_{50}$  values of 21.6  $\pm$  0.6 nM for BD-CsA and 25.8  $\pm$  1.5 nM for NBD-CsA (Fig. 6C). Complete inhibition of transport was observed at >100 nM tariquidar.

#### Monitoring the BD-CsA Efflux from HeLa Cells in a Monolayer by Fluorescence Microscopy

To label the cells with BD-CsA and NBD-CsA and visualize the efflux, HeLa cells transduced with BacMam baculovirus expressing human P-gp were plated in 24-well plates. The monolayer of HeLa cells

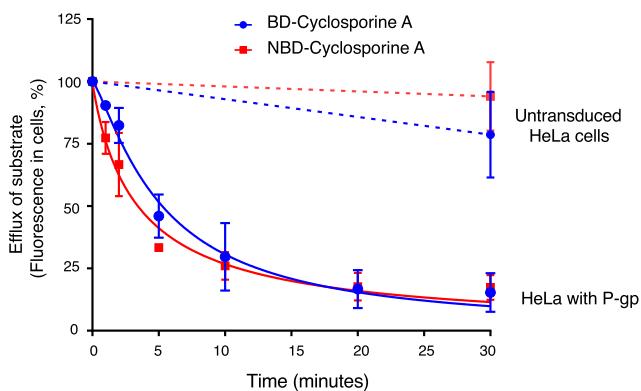


**Fig. 5.** The rate of efflux by human P-gp is similar for BD-CsA and NBD-CsA. Time-dependent efflux of BD-CsA (blue circles) with NBD-CsA (red squares). Fluorescence intensity of untransduced cells and cells expressing human P-gp at the 0 time point was taken as 100%, and relative fluorescence was calculated for 30 minutes. A similar extent of efflux from P-gp-expressing cells was observed for both BD-CsA and NBD-CsA with  $T_{1/2}$  of 5.5  $\pm$  1.5 and 3.4  $\pm$  0.7 minutes, respectively. Untransduced cells did not show significant efflux of either substrate (blue and red dashed lines). The mean values from three independent experiments are given, and error bars show S.D.

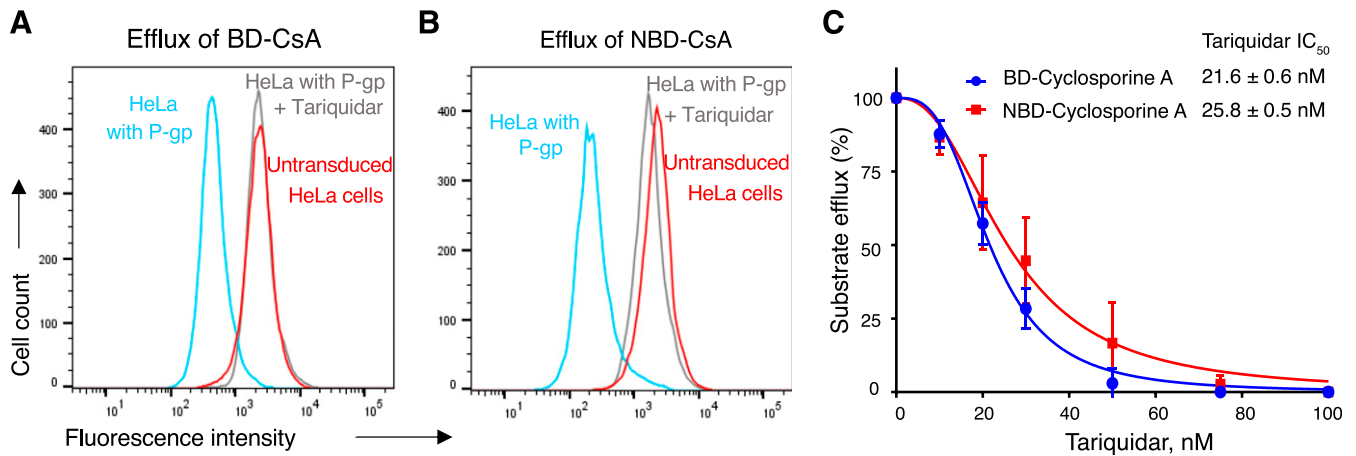


**Fig. 6.** Inhibition of BD-CsA and NBD-CsA transport by tariquidar. Histogram traces showing the steady-state efflux of BD-CsA (A) and NBD-CsA (B) by P-gp (blue traces), and inhibition of efflux by tariquidar (200 nM) (gray traces). The fluorescence intensity was compared with the cells not expressing P-gp (untransduced, red traces). (C) Graph plot showing the tariquidar concentration-dependent inhibition of efflux by P-gp and comparison of BD-CsA (blue circles) with NBD-CsA (red squares). The  $IC_{50}$  for tariquidar was  $21.6 \pm 0.6$  nM for BD-CsA and  $25.8 \pm 1.5$  nM for NBD-CsA. The experiment was repeated three times, and error bars show S.D.

was incubated with BD-CsA and NBD-CsA for 45 minutes, and nuclei were stained with NucBlue. The fluorescence intensity of the cells owing to the presence of NBD-CsA and BD-CsA was determined by using a fluorescence microscope. Untransduced cells showed a higher level of staining with both BD-CsA (Fig. 7) and NBD-CsA (Fig. 8), whereas cells expressing P-gp showed negligible intracellular fluorescence attributable to their efflux. To substantiate these results further, tariquidar was used to block the transport function of P-gp. As evident, the addition of tariquidar increases the cellular fluorescence intensity of both BD-CsA and NBD-CsA, showing efflux of these compounds specifically by P-gp (Figs. 7 and 8).

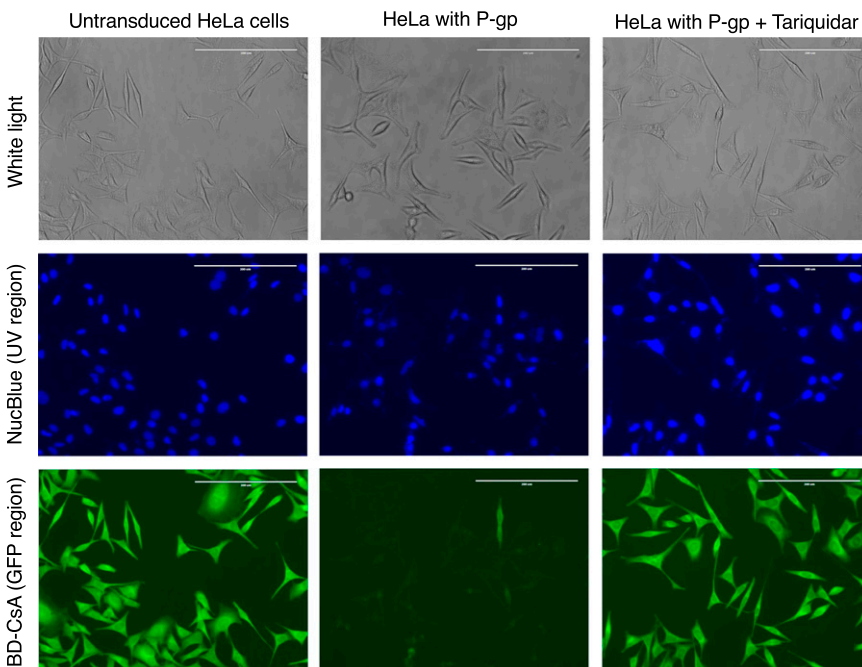
#### Effect of BD-CsA and NBD-CsA on ATPase Activity

Substrates of P-gp usually affect the ability of the transporter to hydrolyze ATP. Some substrates stimulate the ATPase activity, whereas some inhibit it or have no effect. In our previous studies, we have shown

that CsA partially inhibits the ATPase activity of P-gp (Kerr et al., 2001; Vahedi et al., 2017; Sajid et al., 2018). Here, we investigated whether BD-CsA modulates ATPase activity in the same way as NBD-CsA. An ATPase assay was carried out using increasing concentrations of the substrates incubated with the protein at 37°C, and ATP hydrolysis was measured in a colorimetric assay. As shown in Supplemental Fig. S5, both BD-CsA and NBD-CsA inhibit the activity of P-gp ATPase to a similar extent, with maximum inhibition observed to be almost 60% at  $2.5 \mu\text{M}$  and comparable  $IC_{50}$  values of  $30 \pm 2.9$  nM for BD-CsA and  $17 \pm 2.6$  nM for NBD-CsA. Thus, the BD-conjugated probe shows properties similar to those of NBD-conjugated CsA.

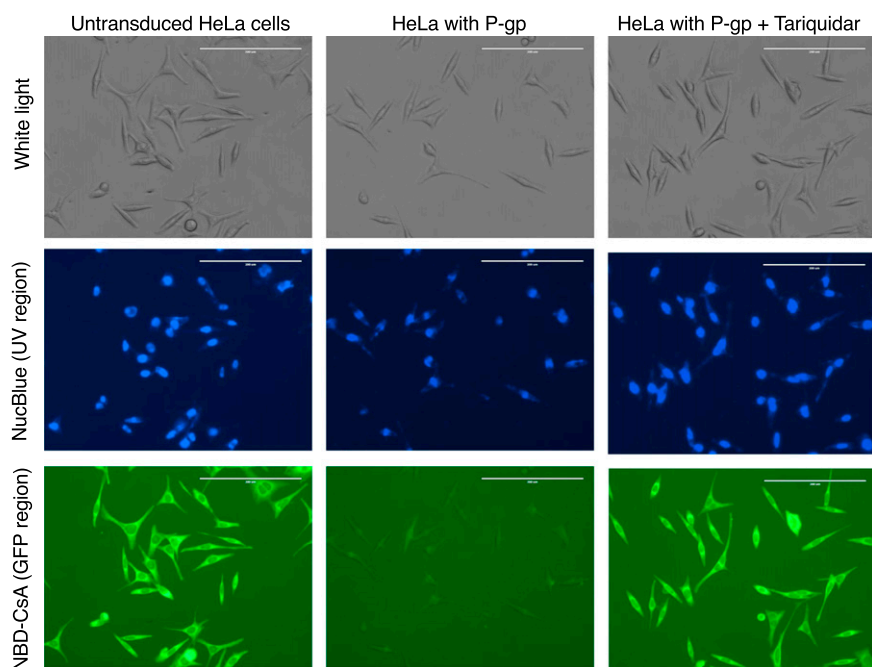
#### Transport of BD-CsA and NBD-CsA by P-gp Mutants

In our previous studies, we generated two mutants of P-gp, named 15Y and TMH1.7. The 15Y mutant has 15 conserved residues in the



**Fig. 7.** Monitoring transport of BD-CsA by fluorescence microscopy. HeLa cells expressing P-gp were used for labeling with BD-CsA and to assess its export by P-gp. After transduction with BacMam baculovirus in 24-well plates, cells in monolayer were incubated with BD-CsA and NucBlue stain (nuclear staining) and visualized using a phase-contrast microscope. Untransduced HeLa cells not expressing P-gp are on the left, HeLa cells expressing P-gp in the center, and HeLa cells expressing P-gp in the presence of 200 nM tariquidar (P-gp inhibitor) are on the right. All three sets were analyzed in transmitted light (top row), NucBlue-stained UV region for visualization of the nucleus (middle row), BD-CsA ( $0.5 \mu\text{M}$ )-stained GFP region (bottom row). All images were taken at original magnification, 10 $\times$ ; scale bar, 200  $\mu\text{m}$ .

Magnification: 10X, bar: 200  $\mu\text{m}$

Magnification: 10X, bar: 200  $\mu\text{m}$ 

**Fig. 8.** Monitoring transport of NBD-CsA by fluorescence microscopy. HeLa cells transduced with P-gp were used for labeling with NBD-CsA and to measure its export by P-gp. After transduction in 24-well plates, cells in monolayer were incubated with 0.5  $\mu\text{M}$  NBD-CsA and NucBlue stains (nuclear staining) and visualized using a phase-contrast microscope. Untransduced HeLa cells not expressing P-gp are on the left, HeLa cells expressing P-gp are in the center, and HeLa cells expressing P-gp with 200 nM tariquidar (P-gp inhibitor) are on the right. All three sets were analyzed in transmitted light (top row); NucBlue-stained UV region for visualization of the nucleus (middle row) and NBD-CsA (0.5  $\mu\text{M}$ )-stained GFP region (bottom row). All images were taken at original magnification 10 $\times$ ; scale bars, 200  $\mu\text{m}$ .

drug-binding pocket substituted with tyrosine. These mutations affect the transport of large (>1000 Da) substrates only, including NBD-CsA, by 15Y mutant P-gp (Vahedi et al., 2017). The TMH1,7 mutant harbors 12 mutations, six in both transmembrane helices 1 and 7, which leads to loss of polyspecificity of the transporter, as it can transport only 3 out of 25 substrates (Sajid et al., 2018), including NBD-CsA. We tested whether these mutants recognize BD-CsA in the same way as NBD-CsA. As shown in Fig. 9A, the 15Y mutant does not efflux either BD-CsA or NBD-CsA (same fluorescence as untransduced cells), whereas TMH1,7 efficiently effluxes both of the probes (>75% efficiency as compared with wild-type P-gp) (Fig. 9B). Thus, BD conjugation does not affect the recognition of CsA by P-gp mutants.

#### Docking of CsA, NBD-CsA, and BD-CsA in the Drug-Binding Pocket of P-gp

To compare the interaction of NBD-CsA and BD-CsA with P-gp, we docked these two molecules and CsA (parent unconjugated compound) in the drug-binding pocket. These studies were carried out with the recently published structure of ligand (Taxol)-bound P-gp (PDB ID:6QEX) as a template. For the purpose of docking, we defined a box that included all the residues in the drug-binding pocket within the transmembrane region of P-gp. AutoDock Vina (Scripps Research Institute) generated a total of nine different poses (Fig. 10). By examining the group of docking poses, we found that for both BD- and NBD-CsA, often the fluorophore was found within the inner leaflet of the membrane, toward the intracellular region. Supplemental Table S1 shows the docking scores for all three ligands. We found that all the poses (for CsA and fluorophore-conjugated CsA) had comparable docking scores for the lowest energy pose (−14.5 kcal/mol). Particularly for CsA, the two lowest energy poses had identical docking scores; however, these poses differed significantly in the relative orientation of CsA, even though they shared many of the interacting residues (data not shown). The high-resolution atomic structure of human P-gp in the presence of paclitaxel (Taxol) revealed a structure in which the ligand could be fitted to the density in more than one orientation, supporting the possibility of different binding modes for the same molecule within the binding site

of P-gp, owing to the flexible nature of the transmembrane region (Alam et al., 2019). This could also be the case for CsA and other molecules. We then focused on the pose with the lowest energy score for each of the molecules. As expected by the large size of the ligand, several amino

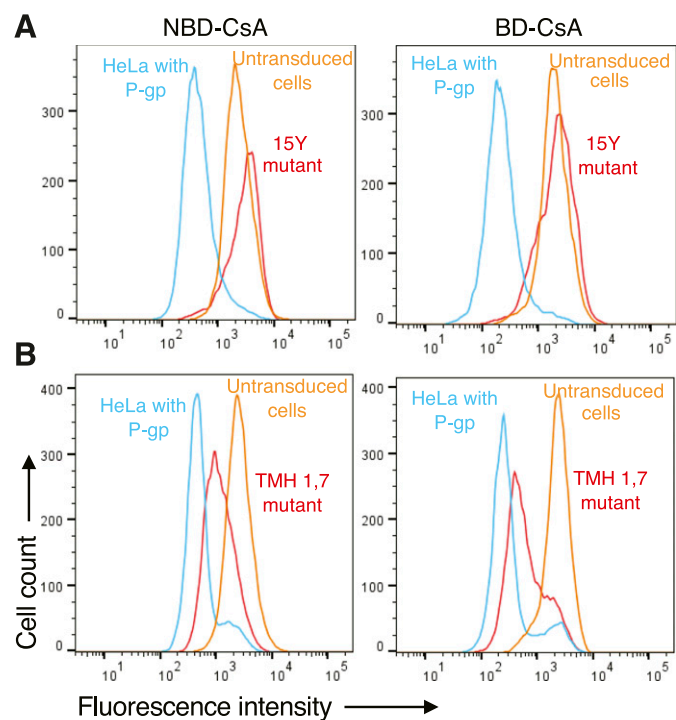


**Fig. 9.** Transport of BD-CsA and NBD-CsA by P-gp mutants. Transport of NBD-CsA (A and B, left) and BD-CsA (A and B, right) by 15Y and TMH 1,7 P-gp mutants. In previous studies, we showed that NBD-CsA is not transported by 15Y (Vahedi et al., 2017), but it is transported by TMH 1,7 mutant P-gp (Sajid et al., 2018). Compared with untransduced cells (not expressing P-gp, orange traces), the fluorescence intensity of HeLa cells expressing P-gp (blue traces) was taken as 100%, and relative transport by mutant P-gp (red traces) was calculated.



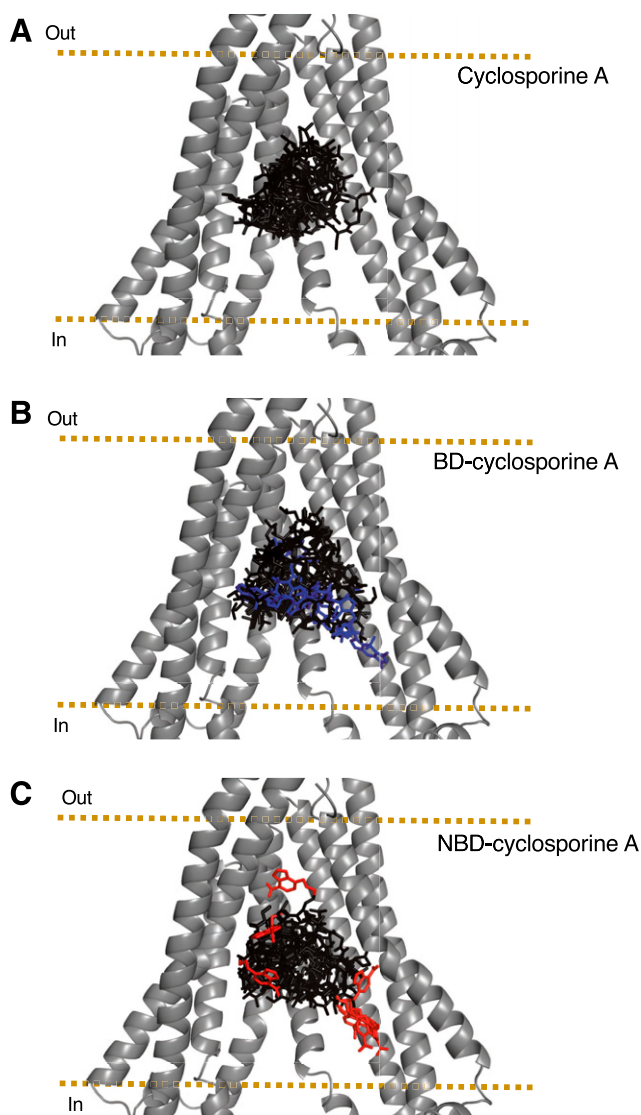


**Fig. 10.** Docking of CsA, BD-CsA, and NBD-CsA in the drug-binding pocket of human P-gp. Cartoon representation of the transmembrane region of human P-gp (PDB ID: 6QEX) in the inward-open conformation and docked ligands (A) CsA, (B) BD-CsA, and (C) NBD-CsA. Transmembrane helices 9–12 were removed for clarity. The fluorophore is highlighted in blue (Bodipy) and red (NBD); the CsA backbone is black. Docking of ligands using the Autodock Vina program, and the cryo-EM structure of human P-gp was performed as described in the *Materials and Methods* section. The image was prepared using Pymol.

acids of P-gp are close enough to interact with the ligands (Supplemental Table S2). Although the relative orientation of the ligands is not the same, they all interact comparably well with residues in the drug-binding pocket of P-gp. We also replaced boron with carbon in the bodipy group for docking of BD-CsA. Although the substitution of boron with carbon has been used by others (Naresh Reddy and Giri, 2016; Verwilt et al., 2017; Zhao et al., 2017; Bonacorso et al., 2018) and by us (Fig. 10), the interaction of boron compared with carbon in the BD-CsA with residues in the drug-binding pocket of P-gp might be different. Resolution of the atomic structure of P-gp bound to BD-CsA would help to resolve this issue.

### Discussion

With the availability of a vast number of fluorescence-based technologies, the use of fluorescent probes in the development of sensitive, as well as quantitative, assays has become common. These assays can be used to

measure multiple types of readouts using techniques such as flow cytometry, microscopy, and spectroscopy. Fluorescently labeled drugs and chemicals are useful for *in vitro* assays to study the functions of proteins, cellular signaling pathways, cell division, labeling of organelles, metabolic functions, nucleotide labeling, etc. These probes are used for *in vivo* research applications as well, such as live cell labeling; intravital imaging; labeling of organs in animal models; localization of tumors, stones, or infections; and labeling of transporters at the blood-brain barrier.

As P-gp is associated with the development of multidrug resistance in cancer, understanding its function is essential. Additionally, P-gp is a highly conserved protein across several species, with homologs present in popular animal models, such as the mouse (87% identity with *Mdr1a*) and zebrafish (64% identity with *Abcb4*). Several *in vitro* and *in vivo* techniques can be used to study different aspects of P-gp, such as expression, topology, transport mechanism, and ATP hydrolysis. As these methods can be applied to a broad range of species to study P-gp, the synthesis of relevant fluorescent substrate probes plays an important part in elucidating the function of this transporter.

CsA, being a cyclic peptide of ~1200 Da, is a unique substrate of P-gp. Therefore, synthesizing its fluorescent conjugate is valuable. Additionally, as P-gp substrates, fluorescent compounds can be useful to study the drug pharmacokinetics, biodistribution, cytotoxicity, and characterization of drug-resistant cancer cell lines. CsA conjugated to an NBD fluorophore has been used as a P-gp substrate in only a limited number of studies. We developed a simplified approach for the synthesis of Bodipy-FL-CsA. Our approach has the advantage that the fluorophore is conjugated during the last synthesis step, allowing the option of introducing other functionalities at the D<sup>8</sup>-lysine, if needed, by a simple amide formation. During synthesis of the CsA conjugates, we made two significant modifications to the reported synthesis of D-Lys-cyclosporine (Eberle and Nuninger, 1993). Thionation, using the pyridine-phosphorous pentasulfide complex (Fig. 2, step B), resulted in a much cleaner thioamide product compared with the reported procedure. During the cyclization step k, the  $\epsilon$ -amine of D-lysine was protected, as its Fmoc derivative provided a UV-positive chromophore, thereby making the separation of the required product easier by using column chromatography.

In this study, we used Bodipy-FL, a well characterized fluorophore, and compared it with NBD, both covalently linked to CsA, a P-gp substrate. Both fluorescent moieties can be excited and detected with similar filter settings ( $\text{NBD}_{\text{ex}} = 468 \text{ nm}$  and  $\text{NBD}_{\text{em}} = 538 \text{ nm}$ ;  $\text{BD}_{\text{ex}} = 470 \text{ nm}$  and  $\text{BD}_{\text{em}} = 520 \text{ nm}$ ), but BD-CsA has sharper emission spectra compared with NBD-CsA (Supplemental Fig. S6). The Bodipy fluorescent group has several advantageous optical properties over NBD. Its long excited-state half-life is useful for fluorescence polarization studies (Ulrich et al., 2008). It has a higher extinction coefficient and quantum yield (extinction coefficient  $>80,000 \text{ cm}^{-1} \text{ M}^{-1}$ ,  $\phi \sim 1.0$ , independent of the solvent); it is more stable, has a smaller Stokes shift, and is relatively easier to synthesize as a conjugated probe (Johnson et al., 1991). In comparison, the NBD moiety has a relatively low extinction coefficient and quantum yield ( $>22,000 \text{ cm}^{-1} \text{ M}^{-1}$ ,  $\phi \sim 0.018$ , in water but increases to 0.3–0.4 in organic solvents). Thus, BD-conjugated chemicals or drugs are brighter and show less to no background noise. In addition, the BD conjugate does not affect the permeability of associated molecules across biologic membranes. These properties are particularly useful for *in vivo* experiments. In past studies, NBD-CsA has been used to study P-gp function in renal tubules and brain capillaries (blood-brain barrier) (Ott et al., 2010; Miller, 2014). It would be beneficial to compare such studies with BD-CsA, with better fluorescence that allows the use of lower concentrations.

We used HeLa cells expressing P-gp after transduction with the BacMam baculovirus to study the transport of BD-CsA. Flow cytometry

and microscopy-based assays were used to compare the kinetics of transport of BD-CsA with NBD-CsA and its inhibition by tariquidar. We show that BD-CsA is a much better probe in terms of its fluorescence intensity, requiring a lower concentration of the compound. Thus, BD-CsA can be used to label live cells, as shown in microscopy-based assays, using concentrations an order of magnitude lower than those of NBD-CsA. The kinetics of transport show that BD-CsA is efficiently exported out of the cells by P-gp with a  $T_{1/2}$  of 5.5 minutes, which is comparable to the NBD-CsA  $T_{1/2}$  of 3.4 minutes.

In our recent studies, we characterized the transport profile of P-gp mutants with altered properties. We found that 15Y mutant P-gp could not transport large substrates, such as NBD-CsA, whereas TMH1,7 mutant P-gp could transport only three of the substrates tested, including NBD-CsA (Vahedi et al., 2017; Sajid et al., 2018). In this study, we observed that the 15Y mutant failed to transport BD-CsA, whereas the TMH1,7 mutant transported it to same extent as NBD-CsA (Fig. 9). Thus, BD-CsA can be used for characterization of P-gp mutants with substitutions in the drug-binding pocket to understand the transport mechanism.

In silico docking experiments show that both BD- and NBD-CsA bind to the substrate-binding pocket in the transmembrane region of P-gp, interacting with numerous residues (Supplemental Table S2). We found that the docking scores are comparable for CsA, BD-CsA, and NBD-CsA, and conjugation of either fluorophore does not interfere with the binding and transport of CsA by P-gp (Fig. 10; Supplemental Table S1). We found that for residues within 5 Å of the ligand (Fig. 10; Supplemental Tables S1 and S2), interaction with the ligand increased with the increase in the molecular weight of the molecule. This included 34 residues for CsA, 42 residues for NBD-CsA, and 46 residues for BD-CsA. In addition, most of the residues that interacted with the parent CsA moiety were shared by all three molecules, whereas the residues that interact with the NBD or BD fluorophores were different.

In conclusion, we synthesized a Bodipy-FL conjugate of CsA and demonstrated that it is a stable probe with high fluorescence yield for monitoring the transport function of P-gp. It has the potential to become the probe of choice for in vivo experiments in animal models, including the mouse and zebrafish.

## Acknowledgments

We thank Kristina Folta and Vivian Lin for technical help and George Leiman for editing the manuscript. The high-performance computational capabilities of the Helix and Biowulf Systems at the National Institutes of Health, Bethesda, were used for docking studies.

## Authorship Contributions

*Participated in research design:* Sajid, Raju, Swenson, Ambudkar.  
*Conducted experiments:* Sajid, Raju, Lusvarghi, Vahedi.  
*Contributed new reagents or analytic tools:* Sajid, Raju, Swenson, Ambudkar.  
*Performed data analysis:* Sajid, Raju, Lusvarghi, Vahedi, Swenson, Ambudkar.  
*Wrote or contributed to the writing of the manuscript:* Sajid, Raju, Lusvarghi, Swenson, Ambudkar.

## References

Alam A, Kowal J, Broude E, Roninson I, and Locher KP (2019) Structural insight into substrate and inhibitor discrimination by human P-glycoprotein. *Science* **363**:753–756.  
 Alam A, Küng R, Kowal J, McLeod RA, Tremp N, Broude EV, Roninson IB, Stahlberg H, and Locher KP (2018) Structure of a zosuquidar and UIC2-bound human-mouse chimeric ABCB1. *Proc Natl Acad Sci USA* **115**:E1973–E1982.  
 Ambudkar SV, Dey S, Hrycyna CA, Ramachandra M, Pastan I, and Gottesman MM (1999) Biochemical, cellular, and pharmacological aspects of the multidrug transporter. *Annu Rev Pharmacol Toxicol* **39**:361–398.  
 Ambudkar SV, Kim IW, and Sauna ZE (2006) The power of the pump: mechanisms of action of P-glycoprotein (ABCB1). *Eur J Pharm Sci* **27**:392–400.  
 Barbarino JM, Staatz CE, Venkataramanan R, Klein TE, and Altman RB (2013) PharmGKB summary: cyclosporine and tacrolimus pathways. *Pharmacogenet Genomics* **23**:563–585.

Bergman J, Pettersson B, Hasimbegovic V, and Svensson PH (2011) Thionations using a P4S10-pyridine complex in solvents such as acetonitrile and dimethyl sulfoxide. *J Org Chem* **76**:1546–1553.  
 Bonacoroso HG, Calheiro TP, Iglesias BA, Acunha TV, Franceschini SZ, Ketzner A, Meyer AR, Rodrigues LV, Nogara PA, Rocha JBT, et al. (2018) 1,1-Difluoro-3-aryl(heteroaryl)-1H-pyrido [1,2-c][1,3,5,2]oxadiazaborinin-9-ium-1-uides: synthesis; structure; and photophysical, electrochemical, and BSA-binding studies. *New J Chem* **42**:1913–1920.  
 Cascorbi I (2011) P-glycoprotein: tissue distribution, substrates, and functional consequences of genetic variations. *Handb Exp Pharmacol* **201**:261–283.  
 Chearwae W, Anuchapreeda S, Nandigama K, Ambudkar SV, and Limtrakul P (2004) Biochemical mechanism of modulation of human P-glycoprotein (ABCB1) by curcumin I, II, and III purified from Turmeric powder. *Biochem Pharmacol* **68**:2043–2052.  
 Chen G, Durán GE, Steger KA, Lacayo NJ, Jaffrézou JP, Dumontet C, and Sikic BI (1997) Multidrug-resistant human sarcoma cells with a mutant P-glycoprotein, altered phenotype, and resistance to cyclosporins. *J Biol Chem* **272**:5974–5982.  
 Chufan EE, Kapoor K, Sim HM, Singh S, Talele TT, Durell SR, and Ambudkar SV (2013) Multiple transport-active binding sites are available for a single substrate on human P-glycoprotein (ABCB1) (Abstract). *PLoS One* **8**:e82463.  
 Chufan EE, Sim HM, and Ambudkar SV (2015) Molecular basis of the polyspecificity of P-glycoprotein (ABCB1): recent biochemical and structural studies. *Adv Cancer Res* **125**:71–96.  
 Demeule M, Laplante A, Murphy GF, Wenger RM, and Béliveau R (1998) Identification of the cyclosporin-binding site in P-glycoprotein. *Biochemistry* **37**:18110–18118.  
 Demeule M, Laplante A, Sepehr-Araé A, Beaulieu E, Averill-Bates D, Wenger RM, and Béliveau R (1999) Inhibition of P-glycoprotein by cyclosporin A analogues and metabolites. *Biochem Cell Biol* **77**:47–58.  
 Dirks NL, Huth B, Yates CR, and Meibohm B (2004) Pharmacokinetics of immunosuppressants: a perspective on ethnic differences. *Int J Clin Pharmacol Ther* **42**:701–718.  
 Eberle MK and Nuninger F (1993) Preparation of [D-cysteine]8-cyclosporin via intramolecular sulfur transfer reaction. *J Org Chem* **58**:673–677.  
 Ejendal KF and Hrycyna CA (2005) Differential sensitivities of the human ATP-binding cassette transporters ABCG2 and P-glycoprotein to cyclosporin A. *Mol Pharmacol* **67**:902–911.  
 Gribar JJ, Ramachandra M, Hrycyna CA, Dey S, and Ambudkar SV (2000) Functional characterization of glycosylation-deficient human P-glycoprotein using a vaccinia virus expression system. *J Membr Biol* **173**:203–214.  
 Gutmann DA, Ward A, Urbatsch IL, Chang G, and van Veen HW (2010) Understanding poly-specificity of multidrug ABC transporters: closing in on the gaps in ABCB1. *Trends Biochem Sci* **35**:36–42.  
 Hartz AM, Miller DS, and Bauer B (2010) Restoring blood-brain barrier P-glycoprotein reduces brain amyloid-beta in a mouse model of Alzheimer's disease. *Mol Pharmacol* **77**:715–723.  
 Jetté L, Beaulieu E, Leclerc JM, and Béliveau R (1996) Cyclosporin A treatment induces over-expression of P-glycoprotein in the kidney and other tissues. *Am J Physiol* **270**:F756–F765.  
 Johnson ID, Kang HC, and Haugland RP (1991) Fluorescent membrane probes incorporating dipyrrometheneboron difluoride fluorophores. *Anal Biochem* **198**:228–237.  
 Jouan E, Le Vée M, Mayati A, Denizot C, Parmentier Y, and Fardel O (2016) Evaluation of P-glycoprotein inhibitory potential using a rhodamine 123 accumulation assay (Abstract). *Pharmaceutics* **8**:E12.  
 Juliano RL and Ling V (1976) A surface glycoprotein modulating drug permeability in Chinese hamster ovary cell mutants. *Biochim Biophys Acta* **455**:152–162.  
 Kelly P and Kahan BD (2002) Review: metabolism of immunosuppressant drugs. *Curr Drug Metab* **3**:275–287.  
 Kerr KM, Sauna ZE, and Ambudkar SV (2001) Correlation between steady-state ATP hydrolysis and vanadate-induced ADP trapping in human P-glycoprotein. Evidence for ADP release as the rate-limiting step in the catalytic cycle and its modulation by substrates. *J Biol Chem* **276**:8657–8664.  
 Kim Y and Chen J (2018) Molecular structure of human P-glycoprotein in the ATP-bound, outward-facing conformation. *Science* **359**:915–919.  
 Li MJ, Nath A, and Atkins WM (2017) Differential coupling of binding, ATP hydrolysis, and transport of fluorescent probes with P-glycoprotein in lipid nanodiscs. *Biochemistry* **56**:2506–2517.  
 Martin C, Berridge G, Mistry P, Higgins C, Charlton P, and Callaghan R (1999) The molecular interaction of the high affinity reversal agent XR9576 with P-glycoprotein. *Br J Pharmacol* **128**:403–411.  
 Masereeuw R, Terlouw SA, van Aubele RA, Russel FG, and Miller DS (2000) Endothelin B receptor-mediated regulation of ATP-driven drug secretion in renal proximal tubule. *Mol Pharmacol* **57**:59–67.  
 Miller DS (2014) Sphingolipid signaling reduces basal P-glycoprotein activity in renal proximal tubule. *J Pharmacol Exp Ther* **348**:459–464.  
 Müller M, Yong M, Peng XH, Petre B, Arora S, and Ambudkar SV (2002) Evidence for the role of glycosylation in accessibility of the extracellular domains of human MRP1 (ABCC1). *Biochemistry* **41**:10123–10132.  
 Muzi M, Mankoff DA, Link JM, Shoner S, Collier AC, Sasongko L, and Unadkat JD (2009) Imaging of cyclosporine inhibition of P-glycoprotein activity using <sup>111</sup>C-verapamil in the brain: studies of healthy humans. *J Nucl Med* **50**:1267–1275.  
 Naaresh Reddy G and Giri S (2016) Super/hyperhalogen aromatic heterocyclic compounds. *RSC Advances* **6**:47145–47150.  
 Nicklisch SC, Rees SD, McGrath AP, Gökirmak T, Bonito LT, Vermeer LM, Cregger C, Loewen G, Sandin S, Chang G, et al. (2016) Global marine pollutants inhibit P-glycoprotein: environmental levels, inhibitory effects, and cocrystal structure (Abstract). *Sci Adv* **2**:e1600001.  
 Ott M, Huls M, Cornelius MG, and Fricker G (2010) St. John's Wort constituents modulate P-glycoprotein transport activity at the blood-brain barrier. *Pharm Res* **27**:811–822.  
 Pawarode A, Shukla S, Minderman H, Fricke SM, Pinder EM, O'Loughlin KL, Ambudkar SV, and Baer MR (2007) Differential effects of the immunosuppressive agents cyclosporin A, tacrolimus and sirolimus on drug transport by multidrug resistance proteins. *Cancer Chemother Pharmacol* **60**:179–188.  
 Pluchino KM, Hall MD, Moen JK, Chufan EE, Fetsch PA, Shukla S, Gill DR, Hyde SC, Xia D, Ambudkar SV, et al. (2016) Human-mouse chimeras with normal expression and function reveal that major domain swapping is tolerated by P-glycoprotein (ABCB1). *Biochemistry* **55**:1010–1023.  
 Ramachandra M, Ambudkar SV, Chen D, Hrycyna CA, Dey S, Gottesman MM, and Pastan I (1998) Human P-glycoprotein exhibits reduced affinity for substrates during a catalytic transition state. *Biochemistry* **37**:5010–5019.

- Saeki T, Ueda K, Tanigawara Y, Hori R, and Komano T (1993) Human P-glycoprotein transports cyclosporin A and FK506. *J Biol Chem* **268**:6077–6080.
- Sajid A, Lusvardi S, Chufan EE, and Ambudkar SV (2018) Evidence for the critical role of transmembrane helices 1 and 7 in substrate transport by human P-glycoprotein (ABCB1). *PLoS One* **13**:e0204693.
- Sanner MF (1999) Python: a programming language for software integration and development. *J Mol Graph Model* **17**:57–61.
- Schramm U, Fricker G, Wenger R, and Miller DS (1995) P-glycoprotein-mediated secretion of a fluorescent cyclosporin analogue by teleost renal proximal tubules. *Am J Physiol* **268**:F46–F52.
- Shen DW, Fojo A, Chin JE, Roninson IB, Richert N, Pastan I, and Gottesman MM (1986) Human multidrug-resistant cell lines: increased mdr1 expression can precede gene amplification. *Science* **232**:643–645.
- Shukla S, Schwartz C, Kapoor K, Kouanda A, and Ambudkar SV (2012) Use of baculovirus BacMam vectors for expression of ABC drug transporters in mammalian cells. *Drug Metab Dispos* **40**:304–312.
- Shukla S, Skoumbourdis AP, Walsh MJ, Hartz AM, Fung KL, Wu CP, Gottesman MM, Bauer B, Thomas CJ, and Ambudkar SV (2011) Synthesis and characterization of a BODIPY conjugate of the BCR-ABL kinase inhibitor Tasigna (nilotinib): evidence for transport of Tasigna and its fluorescent derivative by ABC drug transporters. *Mol Pharm* **8**:1292–1302.
- Storck SE, Hartz AMS, Bernard J, Wolf A, Kachlmeier A, Mahringer A, Weggen S, Pahnke J, and Pietrzik CU (2018) The concerted amyloid-beta clearance of LRP1 and ABCB1/P-gp across the blood-brain barrier is linked by PICALM. *Brain Behav Immun* **73**:21–33.
- Strouse JJ, Ivnitcki-Steele I, Waller A, Young SM, Perez D, Evangelisti AM, Ursu O, Bologna CG, Carter MB, Salas VM, et al. (2013) Fluorescent substrates for flow cytometric evaluation of efflux inhibition in ABCB1, ABCC1, and ABCG2 transporters. *Anal Biochem* **437**:77–87.
- Szewczyk P, Tao H, McGrath AP, Villaluz M, Rees SD, Lee SC, Doshi R, Urbatsch IL, Zhang Q, and Chang G (2015) Snapshots of ligand entry, malleable binding and induced helical movement in P-glycoprotein. *Acta Crystallogr D Biol Crystallogr* **71**:732–741.
- Szöllösi D, Rose-Sperling D, Hellmich UA, and Stockner T (2018) Comparison of mechanistic transport cycle models of ABC exporters. *Biochim Biophys Acta Biomembr* **1860**:818–832.
- Tanaka K, Hirai M, Tanigawara Y, Yasuhara M, Hori R, Ueda K, and Inui K (1996) Effect of cyclosporin analogues and FK506 on transcellular transport of daunorubicin and vinblastine via P-glycoprotein. *Pharm Res* **13**:1073–1077.
- Tedesco D and Haragsim L (2012) Cyclosporine: a review. *J Transplant* **2012**:230386.
- Thiebaut F, Tsuruo T, Hamada H, Gottesman MM, Pastan I, and Willingham MC (1987) Cellular localization of the multidrug-resistance gene product P-glycoprotein in normal human tissues. *Proc Natl Acad Sci USA* **84**:7735–7738.
- Trott O and Olson AJ (2010) AutoDock Vina: improving the speed and accuracy of docking with a new scoring function, efficient optimization, and multithreading. *J Comput Chem* **31**:455–461.
- Ulrich G, Ziessel R, and Harriman A (2008) The chemistry of fluorescent bodipy dyes: versatility unsurpassed. *Angew Chem Int Ed Engl* **47**:1184–1201.
- Vahedi S, Chufan EE, and Ambudkar SV (2017) Global alteration of the drug-binding pocket of human P-glycoprotein (ABCB1) by substitution of fifteen conserved residues reveals a negative correlation between substrate size and transport efficiency. *Biochem Pharmacol* **143**:53–64.
- Vahedi S, Lusvardi S, Pluchino K, Shafirir Y, Durell SR, Gottesman MM, and Ambudkar SV (2018) Mapping discontinuous epitopes for MRK-16, UIC2 and 4E3 antibodies to extracellular loops 1 and 4 of human P-glycoprotein. *Sci Rep* **8**:12716.
- Verwilt P, Kim HR, Seo J, Sohn NW, Cha SY, Kim Y, Maeng S, Shin JW, Kwak JH, Kang C, et al. (2017) Rational design of in vivo tau tangle-selective near-infrared fluorophores: expanding the BODIPY universe. *J Am Chem Soc* **139**:13393–13403.
- Weiss J, Kerpen CJ, Lindenmaier H, Dormann SM, and Haefeli WE (2003) Interaction of antiepileptic drugs with human P-glycoprotein in vitro. *J Pharmacol Exp Ther* **307**:262–267.
- Wenger RM (1986) Cyclosporine and analogues— isolation and synthesis— mechanism of action and structural requirements for pharmacological activity. *Fortschr Chem Org Naturst* **50**:123–136.
- Wenger RM (1988) Cyclosporine: conformation and analogues as tools for studying its mechanism of action. *Transplant Proc* **20** (2 Suppl 2):313–318.
- Yigitaslan S, Erol K, and Cengelli C (2016) The effect of P-glycoprotein inhibition and activation on the absorption and Serum levels of cyclosporine and tacrolimus in rats. *Adv Clin Exp Med* **25**: 237–242.
- Zhao N, Williams TM, Zhou Z, Fronczek FR, Sibrán-Vázquez M, Jois SD, and Vicente MGH (2017) Synthesis of BODIPY-peptide conjugates for fluorescence labeling of EGFR overexpressing cells. *Bioconjug Chem* **28**:1566–1579.

---

**Address correspondence to:** Suresh V. Ambudkar, National Cancer Institute, NIH, Building 37, Room 2120, 37 Convent Drive, Bethesda, MD 20892-4256. E-mail: ambudkar@mail.nih.gov

---

## *Drug Metabolism and Disposition*

*Supplementary Materials for:*

**Synthesis and characterization of BODIPY-FL-cyclosporine A as a substrate for multidrug resistance-linked P-glycoprotein (ABCB1)**

Andaleeb Sajid, Natarajan Raju, Sabrina Lusvardi, Shahrooz Vahedi, Rolf E. Swenson, Suresh V. Ambudkar

**Table S1: Docking scores of the 9 lowest energy poses of CsA, NBD-CsA and BD-CsA docked into human P-gp structure (6QEX.pdb).**

Docking pose number	Docking energy (kcal/mol)		
	CsA	NBD-CsA	BD-CsA
1	-14.5	-14.5	-14.5
2	-14.5	-13.8	-13.8
3	-14.2	-13.8	-13.2
4	-14.1	-13.8	-12.2
5	-13.5	-13.8	-12.1
6	-13.3	-13.8	-12.1
7	-13.2	-13.7	-12.1
8	-13.2	-13.7	-12
9	-13.2	-13.6	-11.9

Autodock Vina program was used for docking ligands in the drug-binding pocket of human P-gp as described in the Materials and Methods Section.

**Table S2: List of amino acid residues present within a 5Å distance of CsA, NBD-CsA and BD-CsA in pose 1 obtained by docking in the drug-binding pocket of human P-gp structure (6QEX.pdb).**

Residues within 5Å of pose 1 for CsA	Residues within 5Å of pose 1 for NBD-CsA	Residues within 5Å of pose 1 for BD-CsA
LEU 65	LEU 65	LEU 65
MET 68	MET 68	MET 68
MET 69	MET 69	MET 69
PHE 72	GLN 195	MET 192
TRP 232	TRP 232	GLN 195
ALA 302	PHE 239	SER 196
PHE 303	ASN 296	THR 199
ILE 306	PHE 303	SER 228
TYR 307	ILE 306	ALA 229
TYR 310	TYR 307	TRP 232
PHE 336	TYR 310	ALA 233
LEU 339	PHE 336	LEU 236
ILE 340	LEU 339	ILE 299
PHE 343	ILE 340	PHE 303
GLN 347	PHE 343	ILE 306
GLN 725	SER 344	TYR 307
PHE 728	GLN 347	TYR 310
PHE 732	ASN 721	PHE 336
GLU 875	GLY 722	LEU 339
MET 876	LEU 724	ILE 340
LEU 879	GLN 725	PHE 343
GLN 946	PHE 728	SER 344

MET 949	PHE 770	GLN 347
TYR 950	GLN 773	ASN 721
TYR 953	SER 831	GLY 722
PHE 957	ALA 834	LEU 724
LEU 975	VAL 835	GLN 725
PHE 978	GLN 838	PHE 728
SER 979	ASN 842	SER 766
VAL 982	GLU 875	PHE 770
PHE 983	MET 876	GLN 773
MET 986	MET 949	GLN 838
ALA 987	TYR 953	ASN 842
GLN 990	SER 979	GLU 875
	PHE 983	MET 876
	MET 986	LEU 879
	ALA 987	GLN 946
	GLN 990	MET 949
	VAL 991	TYR 953
	PHE 994	VAL 982
	ALA 995	PHE 983
	PRO 996	MET 986
		ALA 987
		GLN 990
		VAL 991
		PHE 994

### HPLC trace of 6

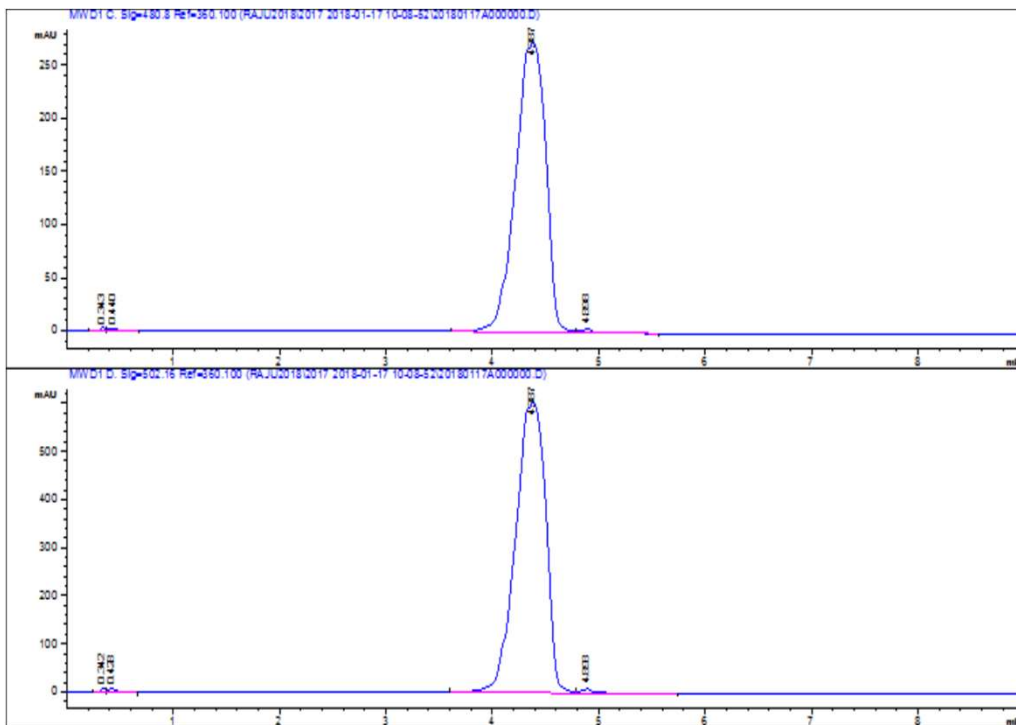


**Figure S1.** HPLC trace of purified BD-CsA: Histogram showing the HPLC trace of compound 6, referring to BD-CsA purity.



### Mass spectrum of 6

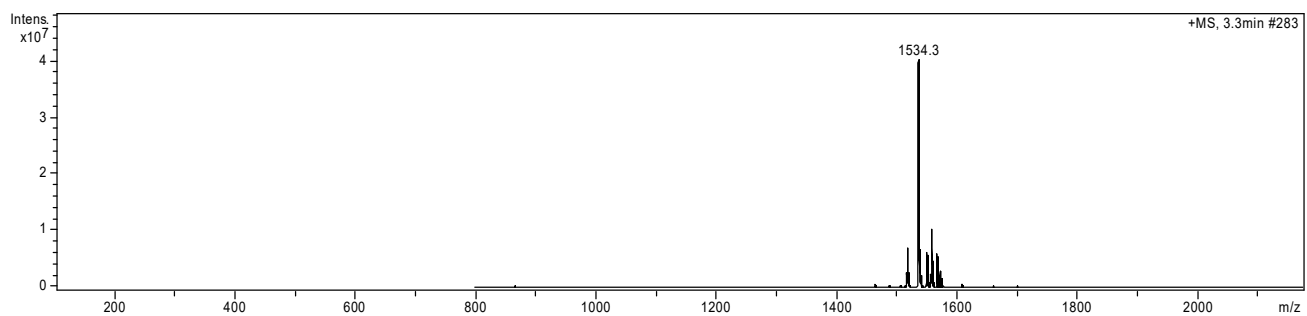


**Figure S2.** Mass spectrum of BD-CsA: Histogram showing MS spectra of compound 6, purified as BD-CsA. The single peak at 1534.3 Da indicates compound purity.

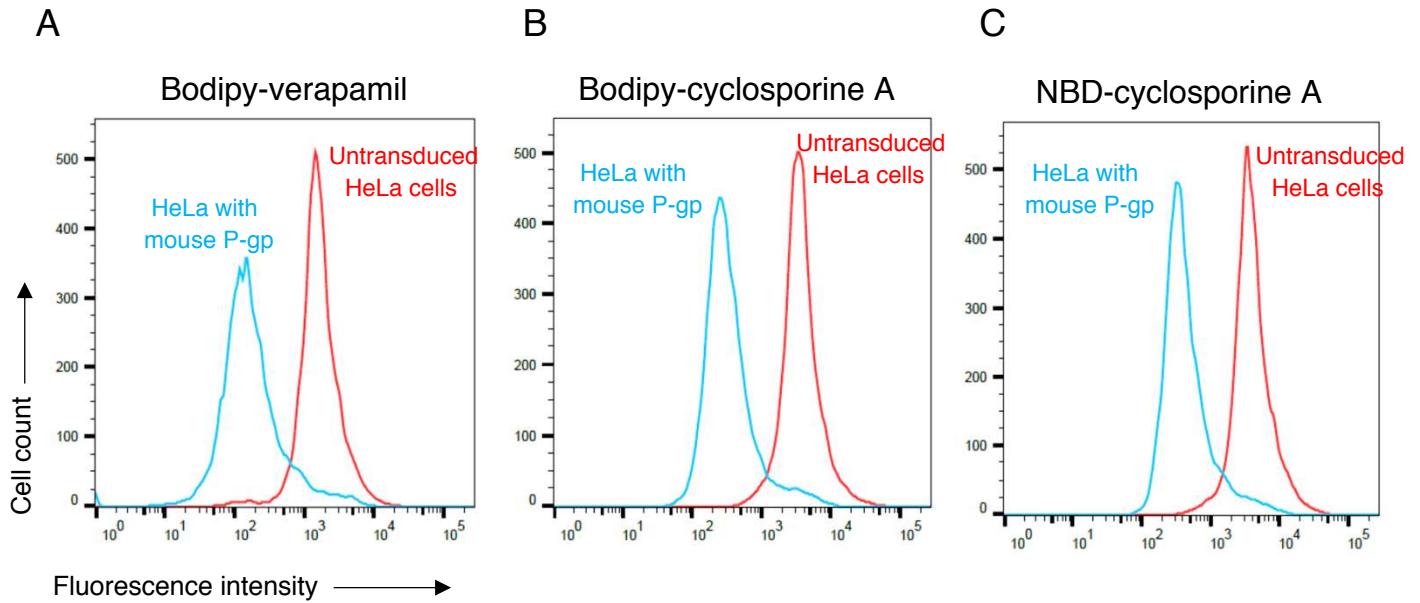


**Figure S3.** BD-CsA is a substrate for mouse P-gp: HeLa cells were transduced with BacMam baculovirus to express mouse P-gp and untransduced cells were used as a control. Cells were incubated with BD-CsA or NBD-CsA ( $0.5 \mu\text{M}$ , each) for 45 minutes at  $37^\circ\text{C}$  and fluorescence was measured using flow cytometry. Histogram traces show the transport of substrates by mouse P-gp, (A) BD-verapamil, (B) BD-CsA and (C) NBD-CsA. The efflux by P-gp was assayed by comparing the fluorescence intensity of cells expressing P-gp (blue traces) with those that do not express P-gp (untransduced cells, red traces).

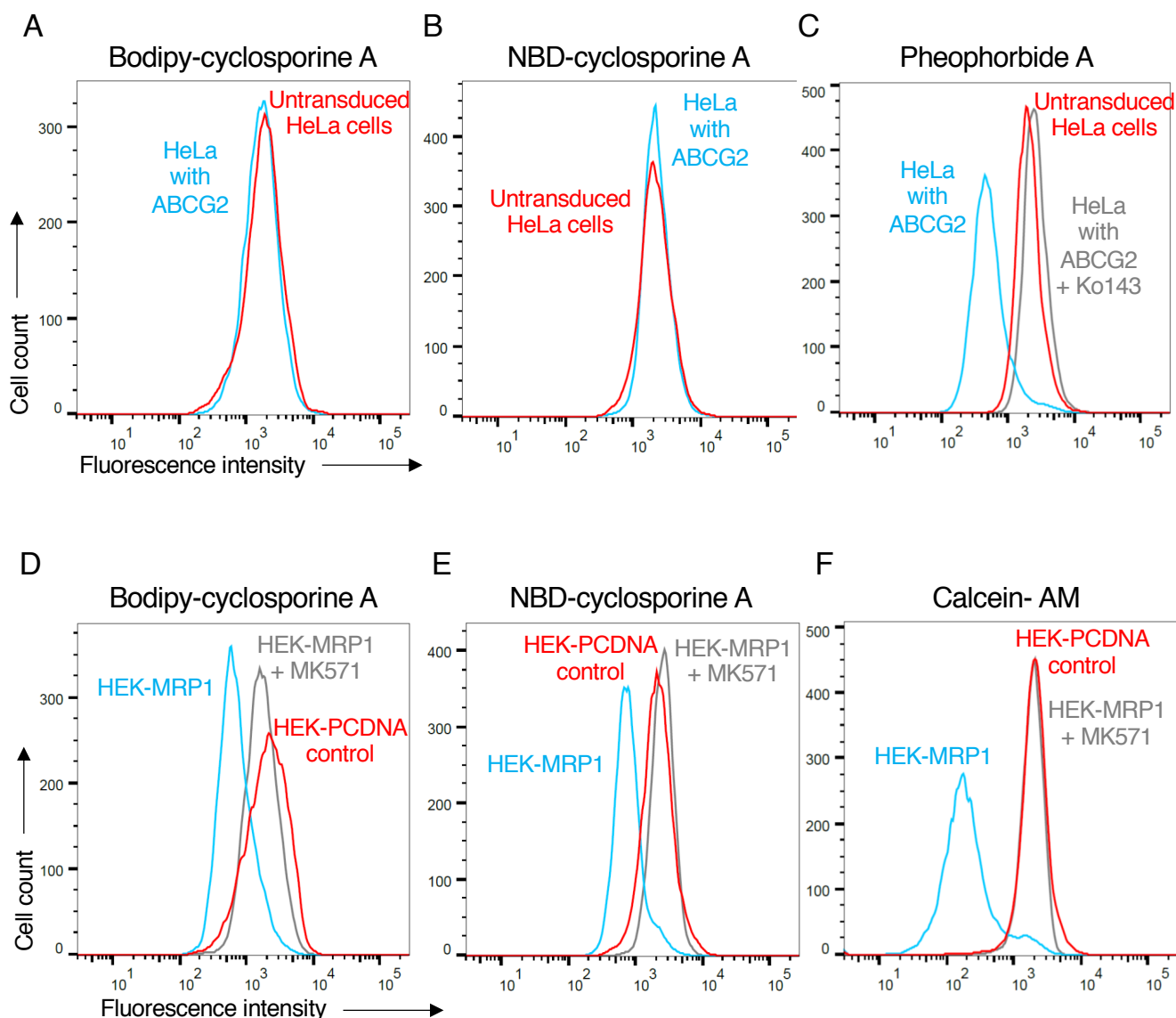


**Figure S4.** Efflux of BD-CsA and NBD-CsA by human ABCG2 and MRP1: (A-C) HeLa cells were transduced with BacMam baculovirus to express human ABCG2 and untransduced cells were used as a control. Cells were incubated with BD-CsA, NBD-CsA ( $0.5 \mu\text{M}$ , each) or pheophorbide A ( $2 \mu\text{M}$ ) for 45 minutes at  $37^\circ\text{C}$  and fluorescence was measured using flow cytometry. Histogram traces show the transport of substrates by ABCG2, (A) BD-CsA, (B) NBD-CsA and (C) Pheophorbide A (known ABCG2 substrate). The ABCG2 inhibitor Ko143 ( $2.5 \mu\text{M}$ ) was used to indicate the specificity of ABCG2. (D-F) HEK-cells transfected with MRP1 or PCDNA3.1 (vector control) were used. Histogram traces show the transport activity of MRP1 with (D) BD-CsA, (E) NBD-CsA and (F) calcein-AM (known MRP1 substrate). The MRP1 inhibitor MK571 was used at  $25 \mu\text{M}$ . The efflux was assayed by comparing the fluorescence intensity of cells expressing the transporter (blue traces) with control (untransduced or parental) cells (red traces). The traces of cells expressing the transporters in the presence of inhibitors are shown in grey.

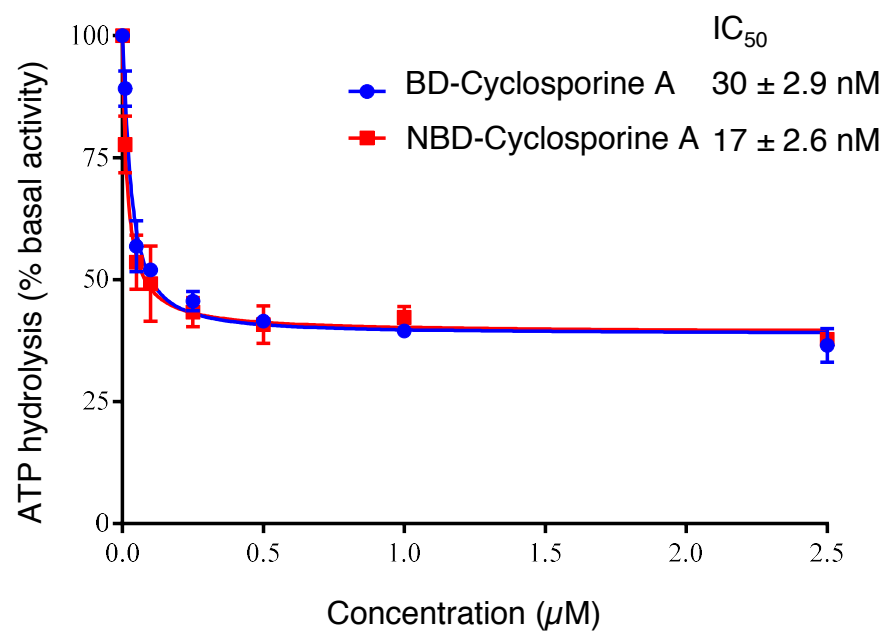
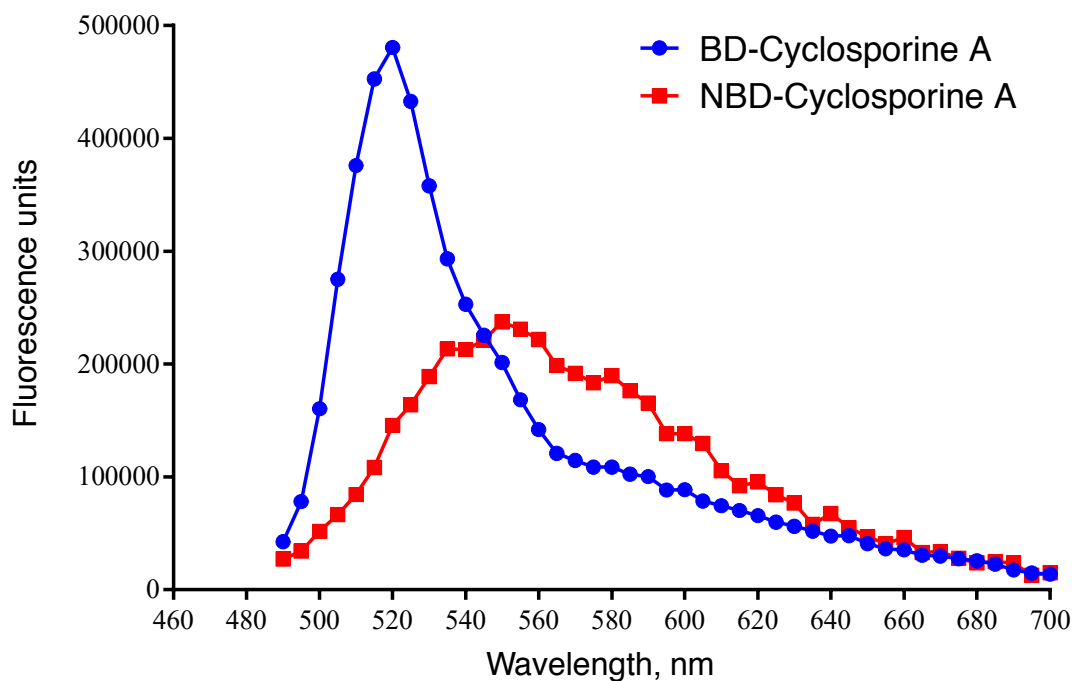


**Figure S5.** Effect of BD-CsA and NBD-CsA on ATPase activity of P-gp: ATPase activity of human P-gp was assayed in insect cell membrane vesicles and the effect of BD-CsA or NBD-CsA at indicated concentrations was measured as described in the Materials and Methods. Both compounds partially inhibited the ATPase activity with IC<sub>50</sub> of 30±2.9 nM for BD-CsA and 17±2.6 nM for NBD-CsA.



Ex. 460 nm

**Figure S6.** Fluorescence emission spectra of BD-CsA and NBD-CsA: Histogram showing the fluorescence emission spectra of BD-CsA (blue circles) and NBD-CsA (red squares), with excitation at 460 nm.